J Neurophysiol
87: 257–272, 2002; 10.1152/jn.00919.2000.

Conjugate and Vergence Oscillations During Saccades and Gaze Shifts: Implications for Integrated Control of Binocular Movement

PIERRE A. SYLVESTRE,[1] HENRIETTA L. GALIANA,[2] AND KATHLEEN E. CULLEN[1]
[1]*Aerospace Medical Research Unit, Department of Physiology and* [2]*Department of Biomedical Engineering, McGill University, Montreal, Quebec H3G 1Y6, Canada*

Received 19 December 2000; accepted in final form 10 October 2001

Sylvestre, Pierre A., Henrietta L. Galiana, and Kathleen E. Cullen. Conjugate and vergence oscillations during saccades and gaze shifts: implications for integrated control of binocular movement. *J Neurophysiol* 87: 257–272, 2002; 10.1152/jn.00919.2000. Saccades made between targets at optical infinity require both eyes to rotate by the same angle. Nevertheless, these saccades are consistently accompanied by transient vergence eye movements. Here we have investigated whether the dynamics of these vergence movements depend on the trajectory of the coincident conjugate movement, and whether moving the head during eye-head gaze shifts modifies vergence dynamics. In agreement with previous reports, saccades with more symmetric (i.e., "bell-shaped") conjugate velocity profiles were accompanied by stereotyped biphasic vergence transients (i.e., a divergence phase immediately followed by a convergence phase). However, we found that saccades with more asymmetric, oscillatory-like dynamics (characterized by a typical conjugate reacceleration of the eyes following the initial peak velocity) were systematically accompanied by more complex vergence movements that also exhibited oscillatory-like dynamics. These findings could be extended to conditions where the head was free to move: comparable conjugate and vergence oscillations were observed during head-restrained saccades and combined eye-head gaze shifts. The duration of the vergence oscillation increased with gaze shift amplitude, such that as many as four vergence phases (divergence-convergence-divergence-convergence) were recorded during 55° gaze shifts (≈240 ms). To quantify these observations, we first determined whether conjugate and vergence peak velocities were systematically correlated. Conjugate peak velocity was linearly related to the peak velocity of the initial divergence phase for saccades and gaze shifts of all amplitudes, regardless of their dynamics. However, for more asymmetric saccades and gaze shifts, the subsequent convergence and divergence peak velocities were not correlated with either the initial peak conjugate velocity or the peak velocity of the conjugate reacceleration. Next, we determined that the duration of the different conjugate and vergence oscillation phases remained relatively constant across all saccades and gaze shifts, and that the conjugate and vergence profiles oscillated together at approximately 7.5–10 Hz. Using computer simulations, we show that a classic feed-forward model is unable to reproduce vergence oscillations based solely on peripheral mechanisms. Furthermore, we demonstrate that small modifications to the gain and delay of a simple feedback model for saccade generation can generate conjugate oscillations, and propose that such changes reflect the influence of lowered alertness on the tecto-reticular pathways. We conclude that peripheral mechanisms can only account for the initial divergence that accompanies all saccades, and that the conjugate and vergence oscillations observed during asymmetric movements arise centrally from an integrative binocular controller.

INTRODUCTION

Conjugate and vergence eye movements are commonly thought to be mediated by separate neural pathways (reviewed by Goldberg 2000). Accordingly, it has been assumed that saccades made between two far targets at optical infinity, for which the two eyes must rotate through the same angle, are driven solely by the conjugate subsystem. In this schema, the drive from the conjugate premotor pathway would provide an identical command to the adducting and abducting oculomotor plants to yoke the binocular eye movements (see Mays 1998). However, recent studies have demonstrated that such saccades are consistently accompanied by transient intrasaccadic vergence movements (the eyes initially diverge, and then subsequently converge) that result from dynamic asymmetries in the right and left eye movements (human: Bruno et al. 1995; Collewijn et al. 1988, 1995, 1997; Eggert and Kapoula 1995; Erkelens et al. 1989; Fioravanti et al. 1995; Oohira 1993; Zee et al. 1992; monkey: Maxwell and King 1992). Collewijn et al. (1988) first described in humans that during saccades, the abducting eye reached higher peak velocities, had more skewed velocity profiles, and moved for a shorter duration than the adducting eye. Further studies (Collewijn et al. 1995, 1997; Maxwell and King 1992) demonstrated that the amplitude of this biphasic vergence transient varied systematically with the metrics of the accompanying saccade (≤25°). Specifically, the peak velocities of both vergence phases increased as a function of peak saccadic conjugate velocity (Maxwell and King 1992) and saccade amplitude (Collewijn et al. 1995, 1997). In addition, the total duration of the vergence transient increased with the duration of the saccade, due primarily to the stretching of the convergence phase (Collewijn et al. 1997).

It has been hypothesized that the differences in abducting and adducting eye dynamics could result from *1*) temporal differences in the premotor drive to the motoneuron pools of both eyes (Maxwell and King 1992; Zee et al. 1992), *2*) mechanical differences in the properties of the abducting and adducting eye plants (Collewijn et al. 1988; Zee et al. 1992), or *3*) central interactions between the saccadic and vergence neu-

Address for reprint requests: K. E. Cullen, McIntyre Medical Research Building, 3655 Drummond St., Rm. 1220, Montreal, Quebec H3G 1Y6, Canada (E-mail: cullen@med.mcgill.ca).

The costs of publication of this article were defrayed in part by the payment of page charges. The article must therefore be hereby marked "*advertisement*" in accordance with 18 U.S.C. Section 1734 solely to indicate this fact.

 0022-3077/02 $5.00 Copyright © 2002 The American Physiological Society

Downloaded from www.physiology.org/journal/jn at Johns Hopkins Univ Serials Dept Electronic (162.129.251.017) on July 26, 2019.

ral subsystems (Collewijn et al. 1988). The first and second hypotheses were directly addressed by Zee and colleagues (1992). Using computer simulations, they demonstrated that intrasaccadic transient vergence velocity profiles could be generated by either mechanism but concluded that the dynamics as well as the duration of the vergence movements were better reproduced by the model based on asymmetries in the oculomotor plant dynamics. Given that the neural mechanisms that control binocular movements are not completely understood (for review, see Leigh and Zee 1999), it is more difficult to evaluate the contribution of central mechanisms to the generation of intrasaccadic transient vergence movements. It has been proposed that an interaction between putative conjugate and vergence premotor pathways could generate transient vergence movements during saccades (Collewijn et al. 1988). Indeed, recent neurophysiological studies have begun to unmask extensive sharing of the premotor circuitry underlying conjugate and vergence eye movements during saccades (Chaturvedi and Van Gisbergen 1999, 2000; Mays and Gamlin 1995a,b; Sylvestre and Cullen 1999b; Zhou and King 1998). To date, the question of whether such an integrated controller contributes to the generation of intrasaccadic transient vergence movements remains to be addressed.

In the present study, we ask the following question: does the fine temporal structure of saccade-related transient vergence movements depend on the accompanying conjugate movement dynamics, and, if so, can this be used to further probe the underlying central mechanisms that coordinate binocular eye movements? Because transient vergence movements have been attributed to the mechanical properties of the eye plant, we first examined whether the initial position of the eyes might alter the dynamics of the vergence profiles. Furthermore, prior studies of transient vergence dynamics have restricted their analysis to saccades with more stereotyped trajectories such as those described as "bell-shaped" by Harris and Wolpert (1998). However, more asymmetric eye movement profiles have been observed in humans and monkeys during large-amplitude saccades (see for example, Bahill and Stark 1975; Cullen and Guitton 1997a) and gaze shifts (Cullen and Guitton 1997b; Cullen et al. 2000; Freedman and Sparks 1997; Phillips et al. 1999; Roy and Cullen 1998). In general, these asymmetric movements exhibit oscillatory-like dynamics in which the initial peak in conjugate eye velocity is followed by a reacceleration. In the present report, we compare the vergence movements that accompanied saccades with bell-shaped dynamics with those that accompanied saccades with more asymmetric dynamics. We also determine whether the vergence transients that accompanied combined eye-head gaze shifts differed from those that accompanied large-amplitude ocular saccades. Finally, using computer simulations, we explore the mechanism(s) underlying the vergence transients described in this report.

METHODS

Two monkeys (*Macaca mulatta*) were prepared for chronic recordings of eye movements using methods that have been previously described (Sylvestre and Cullen 1999a). Briefly, to record gaze position, an 18- to 19-mm diam eye coil (3 loops of Teflon-coated stainless steel wire) was implanted in each eye (Judge et al. 1980). A stainless steel post, which allowed the complete immobilization of the animal's head, was attached to the skull with stainless steel screws and dental acrylic. The surgeries were performed under aseptic conditions, and the animals were given 2 wk to recover before any experiments were performed. All procedures were approved by the McGill University Animal Care Committee, and complied with the guidelines of the Canadian Council on Animal Care.

Experimental protocols

During the experiments, the monkey was comfortably seated in a primate chair that was positioned to orient the monkey's head in the center of a 1-m^3, earth-fixed magnetic field coil system (CNC Engineering). The horizontal and vertical positions of the right and left eyes were recorded using the magnetic search coil technique (Fuchs and Robinson 1966). Eye position signals were sampled on-line at 1 kHz and digitally low-pass filtered at 125 Hz. Conjugate position was defined as the average position of the left and right eyes (conjugate = [left eye + right eye]/2; rightward eye movements are denoted by positive values), and vergence position was defined as the difference between the left and right eye positions (vergence = [left eye − right eye]; positive values indicate convergence). Velocity signals were computed by differentiating the position traces and were digitally low-pass filtered at 60 Hz. A specially designed head-holder (Roy and Cullen 1998) permitted complete restraint of the monkey's head, or alternatively full freedom of head movement in the yaw, pitch, and roll planes. In the latter condition, horizontal head position was recorded using a potentiometer attached to the animal's head post (Spectrol Electronics).

Both monkeys were trained to follow, for a juice reward, a small HeNe laser target that was projected onto a cylindrical screen (i.e., isovergent; ≈3.5° convergence) located 55 cm away from their eyes. During head-restrained experiments, rightward and leftward horizontal saccades (5, 15, 25, and 35°) that either began (centrifugal) or ended (centripetal) at the primary position (when the monkey was looking straight ahead) were elicited by stepping targets between horizontal positions in predictable and unpredictable sequences. In addition, the "barrier" paradigm, in which a real food target (e.g., peanut or raisin) appeared unexpectedly on either side of an opaque screen facing the monkey (Cullen and Guitton 1997a), was utilized to elicit saccades under conditions where the animal was especially attentive to the target. During head-unrestrained experiments, rightward and leftward horizontal gaze shifts (35, 45, and 55°) were elicited by presenting laser targets in predictable and unpredictable sequences, and by use of the "barrier" paradigm. During the experiments, the laser targets, the on-line data displays, and the data acquisition were controlled using REX, a QNX-based real-time acquisition system (Hayes et al. 1982). Off-line analysis was performed using custom algorithms written in Matlab (Mathworks).

Data analysis

For saccades and gaze shifts, conjugate movement onset and offset was determined using a 20°/s velocity criterion. Because vergence movements were slower than conjugate movements and often terminated with a slow velocity tail, vergence onset and offset were defined as the time at which the vergence velocity first crossed 5°/s and then remained above (onset) or below (offset) 5°/s for ≥10 ms. Only saccades and gaze shifts that had net changes in vertical eye positions <2.5° were considered to be horizontal movements. Gaze shifts for which the head contributed <10% of the total amplitude were not included in the analysis.

Saccades and gaze shifts were analyzed separately based on their amplitude (5, 15, 25, and 35° for saccades; 35, 45, and 55° for gaze shifts). Average saccade or gaze shift trajectories were computed after 20–30 trials of comparable amplitudes and dynamics were aligned on conjugate movement onset. Statistical analysis was performed using standard bivariate and multivariate linear regression techniques, and

Downloaded from www.physiology.org/journal/jn at Johns Hopkins Univ Serials Dept Electronic (162.129.251.017) on July 26, 2019.

Student's *t*-tests. Unless otherwise specified, all reported values represent means ± SD.

RESULTS

In this section, we first characterize intrasaccadic vergence eye movements for small (<25°) symmetric bell-shaped saccades and specifically compare the intrasaccadic vergence movements that accompany centrifugal and centripetal saccades. We then characterize the vergence movements that accompany larger amplitude bell-shaped and asymmetric saccades to determine whether the intrasaccadic vergence response depends on the dynamics of the conjugate velocity profile. Finally, we compare the transient vergence eye movements that are generated during head-unrestrained combined eye-head gaze shifts with those generated during head-restrained saccades of similar amplitudes. Note that *all* the gaze movements described here were made between isovergent targets.

Vergence transients during small amplitude saccades

Figure 1, *A* and *B*, shows examples of typical 5 and 15° rightward saccades, respectively, for *monkey J*. Conjugate and vergence position traces are shown in the *leftmost panels*, and the corresponding conjugate and vergence velocity traces are shown in the *middle* and *rightmost panels*, respectively. In each panel, the thicker black solid trace represents the average movement profile, and the thin gray traces represent individual saccades aligned on conjugate movement onset (see METHODS). Both animals consistently generated comparable duration eye movements for each saccade amplitude [*monkey J* (mean duration ± SD): 29 ± 3 and 56 ± 9 ms; *monkey B*: 29 ± 2 and 48 ± 6 ms, for 5 and 15° saccades, respectively]. These saccades were characterized by smooth and fairly symmetric acceleration and deceleration phases that resulted in the bell-shaped conjugate velocity profiles shown in Fig. 1. The vergence transient that accompanied each of these saccades had a stereotyped biphasic velocity profile; it was characterized by an initial short-lasting divergence phase (*monkey J*: 17 ± 3 and 23 ± 4 ms; *monkey B*: 22 ± 2 and 28 ± 5 ms, for 5 and 15° saccades, respectively) which was immediately followed by a convergence phase (*monkey J*: 30 ± 6 and 52 ± 5 ms; *monkey B*: 32 ± 7 and 40 ± 13 ms, for 5 and 15° saccades, respectively). The later convergence phase consistently ended after the saccade (arrows in Fig. 1). Similar vergence transients have been previously described for saccades of comparable amplitudes and durations (Collewijn et al. 1988, 1995, 1997; Maxwell and King 1992; Oohira 1993; Zee et al. 1992).

A comparison of the vergence velocity profiles that accompanied 5 versus 15° saccades (Fig. 1) suggests that peak divergence and convergence velocities increase as a function of saccade amplitude and/or velocity. We quantified the relationship between peak vergence (divergence and convergence) and peak conjugate velocity for short-duration (<100 ms) saccades with amplitudes between 5 and 25° (Fig. 2). In agreement with Maxwell and King (1992), significant relationships were observed between the peak conjugate velocity and the initial divergence peak velocity [$R = 0.87$ (Fig. 2*A*) and 0.92 (Fig. 2*C*), *monkey J* and *B*, respectively] as well as the following convergence peak velocity [$R = 0.80$ (Fig. 2*B*) and 0.89 (Fig. 2*D*), *monkey J* and *B*, respectively]. Larger slopes were obtained for the divergence peak than for the convergence peak (0.25 vs. 0.09, and 0.17 vs. 0.13, for *monkey J* and *B*, respectively).

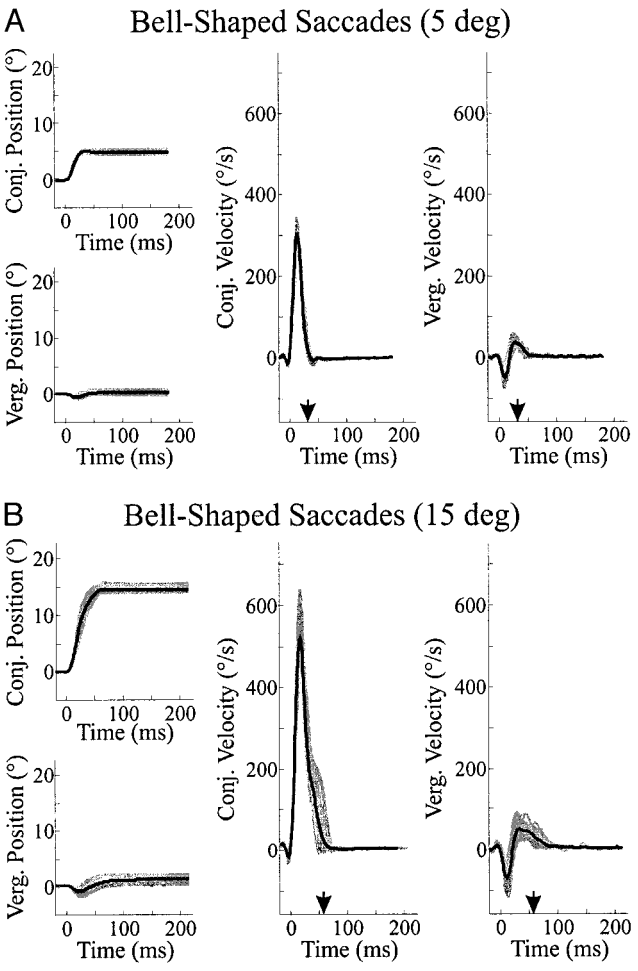

FIG. 1. Typical examples of small-amplitude saccades for *monkey J*. *A*: 5° saccades were accompanied by a biphasic (divergence-convergence) vergence transient. Conjugate and vergence instantaneous positions (*leftmost column*, *top* and *bottom panels*, respectively) and velocities (*middle* and *rightmost panels*, respectively) are plotted as a function of time. All traces are aligned on the onset of the conjugate movement. Average position and velocity profiles (black solid curves) are superimposed on the individual saccadic profiles (thin gray curves, $n = 41$). The arrows indicate the end of the average conjugate movement. Positive conjugate positions are to the right of the primary position (i.e., when the monkey looks straight ahead), and positive vergence positions indicate convergence of the eyes. *B*: 15° saccades were also accompanied by biphasic vergence transients ($n = 26$).

To verify that the recorded vergence velocity profiles did not result, in part, from the improper calibration of one eye coil relative to the other, we compared the average traces obtained for rightward and leftward saccades of comparable amplitudes, durations, peak conjugate velocities, and initial conjugate positions. The improper calibration of one eye coil versus the other would produce an initial divergent velocity during saccades in one direction, and an initial convergent velocity during saccades in the other (Maxwell and King 1992). However, as is illustrated in Fig. 3, rightward and leftward saccades were accompanied by an initial divergent velocity, and furthermore, the intrasaccadic vergence dynamics were virtually identical for both directions (Fig. 3, *A* and *B*, for *monkeys J* and *B*,

Downloaded from www.physiology.org/journal/jn at Johns Hopkins Univ Serials Dept Electronic (162.129.251.017) on July 26, 2019.

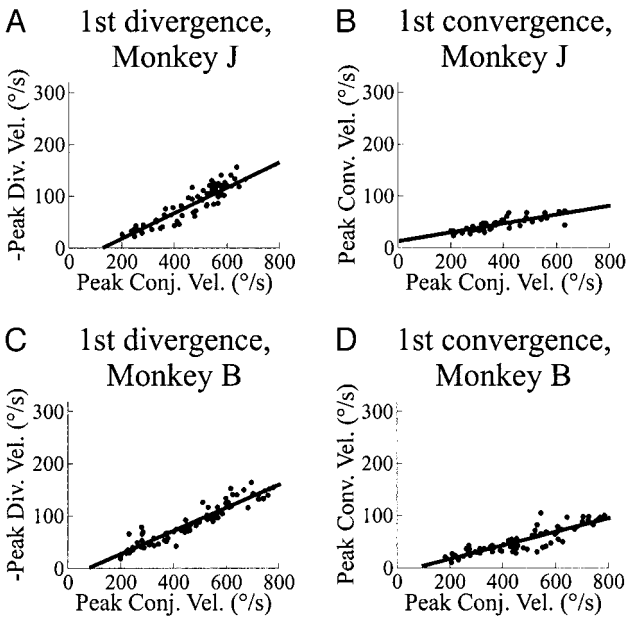

FIG. 2. Relationship between peak vergence and conjugate velocities during small amplitude saccades. *A* and *B*: for *monkey J*, the peak conjugate velocity of small symmetric saccades (5–25°) was well correlated with (*A*) the peak divergence, and (*B*) the peak convergence of the vergence transients. *C* and *D*: for *monkey B*, the peak conjugate velocity of small symmetric saccades (5–25°) was also well correlated with (*C*) the peak divergence, and (*D*) the peak convergence of the vergence transients. Note that to simplify comparison of the divergence and convergence relationships, the sign of the peak divergence velocities has been inverted.

respectively; also see *insets*). The similarity in the intrasaccadic vergence velocities that accompanied leftward and rightward directed saccades further indicates that neither eye was tethered by the eye coil lead as it laterally exited the orbit; had one of the eyes been tethered, its motion would have differed during adduction versus abduction, thereby generating vergence transients with different dynamics depending on the direction of the saccade.

Vergence transients during centrifugal versus centripetal saccades

The dynamics of biphasic vergence transients were also characterized for saccades of equal amplitudes and directions that began from different initial eye positions. Figure 4 shows the conjugate and vergence profiles associated with 15° rightward saccades that started at the primary position (centrifugal conjugate movement; *A*), and that started eccentrically and ended at the primary position (centripetal conjugate movement; *B*), for *monkey J.* As is exemplified in the *inset* of Fig. 4*B*, we found that the timing of the different vergence velocity features was unaffected by the initial eye position, but that the amplitude of both the divergent and the convergent peaks was smaller when associated with centrifugal saccades ($P < 0.05$). These differences in peak divergence and convergence velocities could be accounted for by the significantly ($P < 0.05$) slower peak conjugate velocities of centrifugal versus centripetal saccades (*monkey J*: 489 ± 43 vs. 560 ± 51°/s; *monkey B*: 503 ± 51 vs. 570 ± 55). Using the relationships shown in Fig. 2, we found that the differences in peak divergence and convergence velocities could be predicted based on the peak conjugate velocities that were generated during both saccade types.

Vergence movements during larger amplitude saccades and gaze shifts

We next characterized the vergence movements that accompanied larger amplitude saccades and gaze shifts. Results were comparable for both monkeys. Consequently, we first illustrate examples for *monkey J* only (Figs. 5–9), and then present a summary of the complete data sets obtained for both monkeys (Figs. 10 and 11).

LARGE-AMPLITUDE SACCADES. Larger amplitude saccades (e.g., 25°) could be accomplished by fairly symmetric, more bell-shaped, conjugate velocity movements (Fig. 5*A*) similar to those of smaller amplitude saccades, as well as by longer

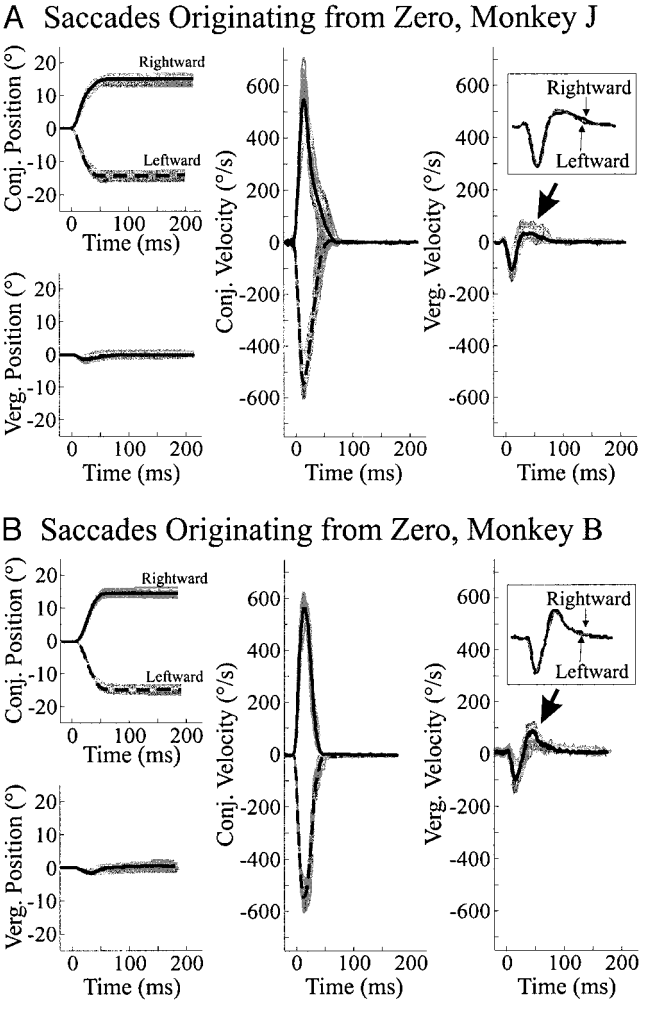

FIG. 3. Similar vergence velocity profiles were associated with rightward and leftward saccades originating from the primary position. *A*: position and velocity profiles associated with rightward ($n = 26$) and leftward ($n = 32$) 15° saccades are shown for *monkey J.* Average traces are superimposed (solid and dashed black curves, for rightward and leftward saccades, respectively). *Inset*: superimposed average vergence velocity profiles for rightward (black curve) and leftward (gray curve) saccades. *B*: position and velocity profiles associated with rightward ($n = 22$) and leftward ($n = 22$) 15° saccades, for *monkey B.* The conventions used were the same as those used in *A*. For both monkeys, the vergence velocity profiles associated with rightward and leftward saccades were comparable.

Downloaded from www.physiology.org/journal/jn at Johns Hopkins Univ Serials Dept Electronic (162.129.251.017) on July 26, 2019.

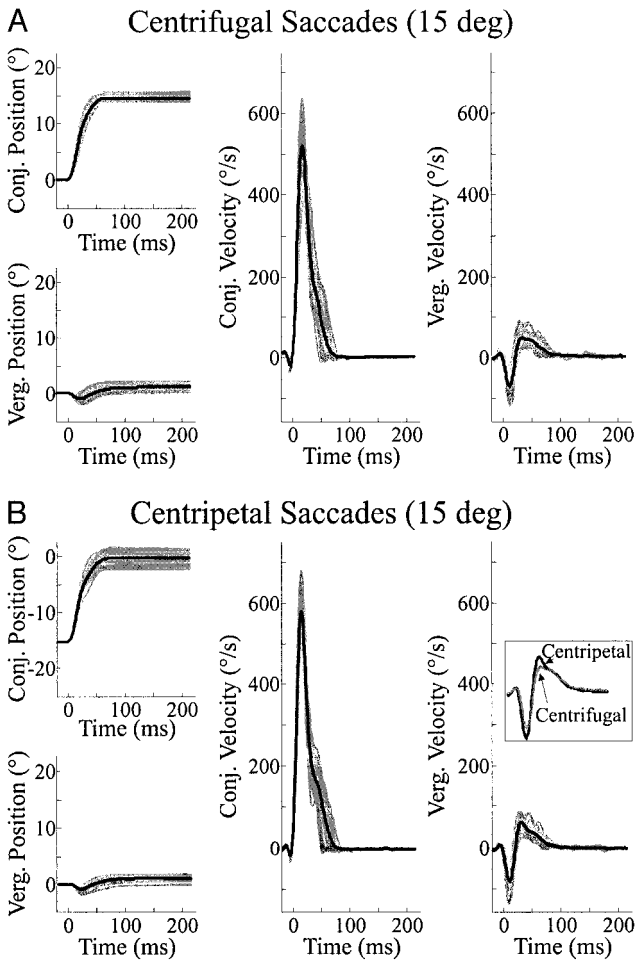

FIG. 4. Effect of initial conjugate eye position on the dynamics of vergence transients. *A*: position and velocity profiles for 15° rightward saccades that originated from the primary position and ended eccentrically (i.e., centrifugal, $n = 26$). *B*: position and velocity profiles for rightward saccades (15°) that started eccentrically and ended at the primary position (i.e., centripetal, $n = 22$). *Inset*: superimposed average vergence velocity profiles associated with centrifugal (gray curve) and centripetal (black curve) saccades. Centripetal saccades were accompanied by faster peak conjugate, divergence, and convergence velocities. Traces are shown for *monkey J*.

duration movements with more asymmetric velocity profiles. In general, this latter class of saccades had slower peak conjugate velocities that were followed by a characteristic reacceleration of the eyes, hence resulting in the oscillatory-like profiles shown in Fig. 5*B*. Furthermore, they had significantly ($P < 0.05$) longer durations than more symmetric movements (165 ± 16 vs. 84 ± 6 ms, and 136 ± 32 vs. 64 ± 7 ms, for *monkeys J* and *B*, respectively). Interestingly, we found that the vergence velocity profiles associated with asymmetric saccades exhibited similar oscillatory-like dynamics (Fig. 5*B*). Indeed, a second divergence phase followed the regular biphasic vergence transient (Fig. 5*B*, *rightmost panel*). This additional second divergent phase did not affect the conjugacy of the saccade, since the average net change in vergence angle at the end of the vergence movement was comparable to that of more symmetric saccades of same amplitude ($P > 0.05$).

We next investigated whether the appearance of the second divergence phase during asymmetric saccades resulted from *1*) the presence of an oscillation in the conjugate velocity profile, *2*) the longer durations of the saccades, or *3*) a combination of both factors. To dissociate the effect of the duration from that of the dynamics, we took advantage of the fact that both monkeys occasionally generated larger amplitude saccades (35°) that had durations comparable to those of smaller asymmetric saccades (25°), but that did not have oscillatory-like conjugate dynamics. Examples of such saccades (35°, 168 ± 15 ms) are shown in Fig. 6*A*. The vergence velocity profiles associated with these saccades were biphasic. Furthermore, the properties of these biphasic transients were well matched with those of smaller amplitude saccades. Specifically, we found that the initial divergence peak velocity remained well correlated ($R = 0.84$) to the maximum conjugate velocity of the accompanying saccades (Fig. 7*A*, gray filled triangles). When we superimposed the regression line computed for the biphasic vergence transients accompanying smaller saccades (see Fig. 2*A*, *monkey J*) on the relationship shown in Fig. 7*A*, a good fit was observed; the slopes of the two regression lines were not statistically different (H_0: $\beta_1 = \beta_2$; $P > 0.05$). Similarly, peak convergence velocities were correlated with peak conjugate velocities (Fig. 7*B*, gray filled triangles: $R = 0.53$), and the slope of this relationship was statistically identical to that

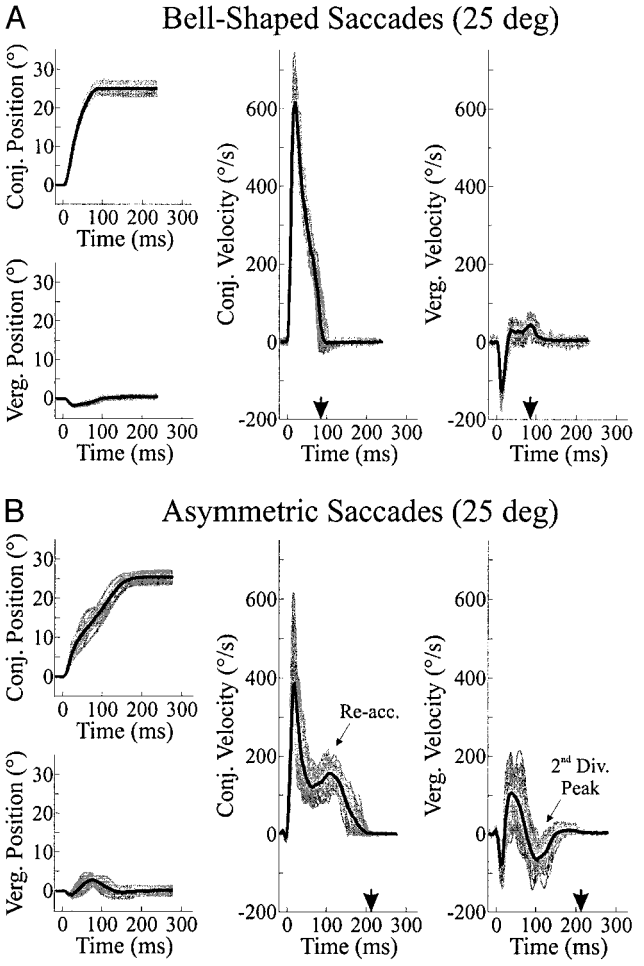

FIG. 5. Vergence movements associated with 25° saccades with symmetric and asymmetric dynamics for *monkey J*. *A*: biphasic vergence velocity profiles were associated with short-duration saccades ($n = 32$). *B*: an additional divergence phase (2nd Div. Peak, *rightmost panel*) followed the regular biphasic transient during similar amplitude saccades with asymmetric dynamics ($n = 25$). Also note the typical reacceleration (Re-acc., *middle panel*) in the conjugate velocity profiles.

Downloaded from www.physiology.org/journal/jn at Johns Hopkins Univ Serials Dept Electronic (162.129.251.017) on July 26, 2019.

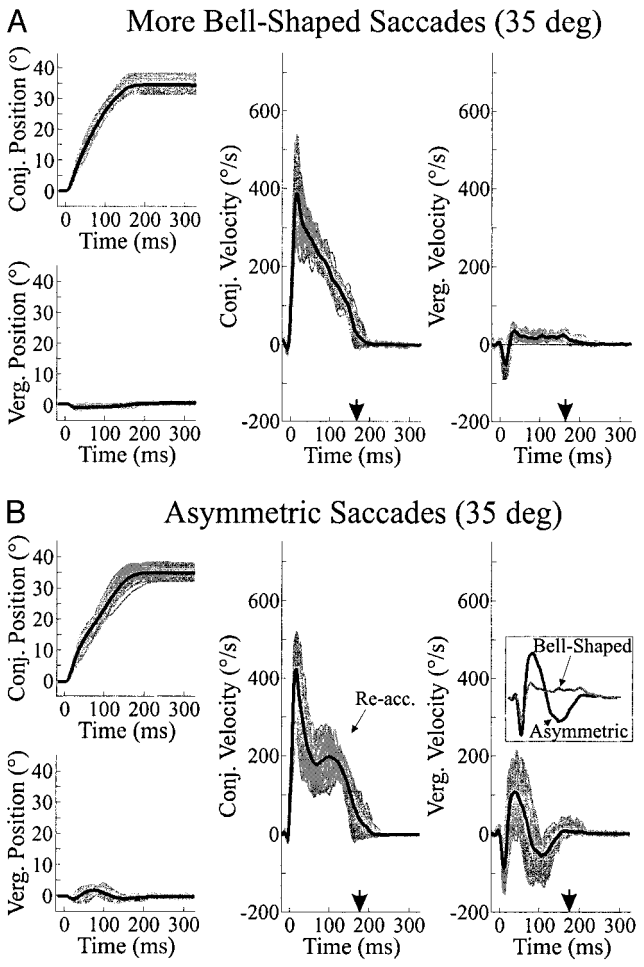

FIG. 6. Vergence movements associated with 35° saccades with more symmetric and asymmetric dynamics, and of comparable duration (*monkey J*). *A*: biphasic vergence velocity profiles were associated with more symmetric saccades ($n = 28$). *B*: in contrast, an additional divergence phase followed the regular biphasic transient elicited during more asymmetric saccades ($n = 31$). *Inset*: superimposed average vergence velocity profiles for 35° saccades with more symmetric (gray curve) and asymmetric (black curve) dynamics.

observed for smaller saccades ($P > 0.05$). Comparable results were obtained for *monkey B* and are included in the legend of Fig. 7.

The results illustrated in Fig. 6*A* indicate that increasing the duration of saccade alone is not sufficient to elicit triphasic vergence movements. Accordingly, we next characterized the intrasaccadic vergence movements that accompanied asymmetric saccades of the same amplitude (35°) and comparable duration (180 ± 16 ms, $P > 0.05$; Fig. 6*B*). As for smaller amplitude asymmetric saccades (e.g., Fig. 5*B*), a second divergence phase consistently followed the initial biphasic transient. The marked differences between the vergence velocity profiles associated with saccades with and without oscillatory dynamics are emphasized in the *inset* of Fig. 6*B*. Furthermore, as shown in Fig. 7*A* (black filled squares), the maximum velocity of the first divergence peak in these triphasic vergence movements was well correlated ($R = 0.78$) with the peak conjugate velocity of saccades. Indeed, this relationship was not significantly different ($P > 0.05$) from that observed for more symmetric saccades (i.e., Fig. 7*A*, gray filled triangles and black filled squares superimpose). However, as shown in Fig. 7*B* for asymmetric saccades (black filled squares), no relationship was observed between the peak velocity of the first convergent phase and the peak conjugate velocity ($R = -0.13$, $P > 0.05$). Similarly, no significant relationship ($R = 0.26$, $P > 0.05$) was observed between the maximum velocity of the divergence phase that followed and the conjugate velocity of the saccade (Fig. 7*C*, black filled squares). Comparable results were obtained for *monkey B* (see legend of Fig. 7). Finally, because the conjugate reacceleration (Fig. 6*B*, *middle panel*) and the second divergence phase occurred roughly simultaneously, we asked whether their peak velocities were correlated, and found that they were not ($R = 0.06$, $P > 0.05$).

Taken together, the above results show that the vergence velocity profiles that accompany saccades vary with the dynamics of the conjugate eye movements: asymmetric saccades

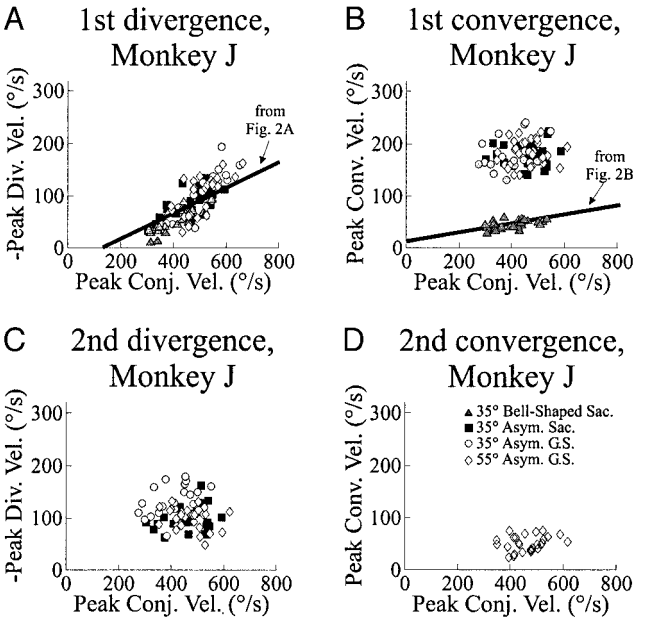

FIG. 7. Relationship between peak vergence and conjugate velocities during large amplitude saccades and gaze shifts, for *monkey J*. *A*: for all saccades and gaze shifts, the peak velocity of the 1st divergence phase was well correlated with the peak conjugate velocity. Thirty-five degree saccades with more symmetric (gray filled triangles) and asymmetric (black filled squares) dynamics, and 35° (gray filled circles) and 55° (open diamonds) gaze shifts are illustrated. To facilitate comparison, the thick solid line shows the regression line obtained in Fig. 2*A* for smaller amplitude symmetric saccades. *B*: the peak convergence velocity was correlated with the peak conjugate velocity during 35° saccades with more symmetric dynamics, but not during more asymmetric saccades and gaze shifts. The thick solid line shows the regression line obtained in Fig. 2*B* for smaller amplitude symmetric saccades. *C* and *D*: neither the 2nd divergence (*C*) nor the 2nd convergence phase (*D*) that accompanied more asymmetric saccades and gaze shifts had their peak velocities correlated with the peak conjugate velocity. Note that similar trends were also observed for *monkey B* (not shown): *1*) peak conjugate velocity vs. peak velocity of the 1st divergence phase: $R = 0.60, 0.44, 0.86, 0.73$ (all significant, $P < 0.05$) for 35° symmetric saccades, 35° asymmetric saccades, and 35 and 55° gaze shifts, respectively. All slopes were statistically the same as that obtained for smaller amplitude symmetric saccades ($P > 0.05$); *2*) peak conjugate velocity vs. peak velocity of the 1st convergence phase: $R = 0.34, -0.22, -0.08, -0.38$ (all nonsignificant, $P > 0.05$), for 35° symmetric saccades, 35° asymmetric saccades, and 35 and 55° gaze shifts, respectively. For symmetric saccades, the data points clustered around the regression line obtained for shorter symmetric saccades; *3*) peak conjugate velocity vs. peak velocity of the 2nd divergence peak: $R = -0.04, 0.42, -0.20$ (all nonsignificant, $P > 0.05$) for 35° asymmetric saccades, and 35 and 55° gaze shifts, respectively; *4*) peak conjugate velocity vs. peak velocity of the 2nd convergence peak: $R = -0.02$ (nonsignificant, $P > 0.05$), for 55° gaze shifts.

Downloaded from www.physiology.org/journal/jn at Johns Hopkins Univ Serials Dept Electronic (162.129.251.017) on July 26, 2019.

with oscillatory-like dynamics are accompanied by triphasic vergence movements that also exhibit oscillatory-like dynamics, whereas stereotyped saccades with more bell-shaped profiles are accompanied by biphasic vergence transients. Since both the conjugate and the vergence dynamics observed during more asymmetric saccades had an oscillatory-like nature, we next investigated whether additional vergence phases would appear during longer lasting movements. In fact, we predicted that a fourth phase (i.e., an additional convergence phase) might be unmasked during asymmetric saccades with durations ≈210–230 ms. However, since neither monkey reliably executed single-step saccades of such durations, we released the monkey's head so that it could generate larger amplitude (and longer duration) combined eye-head gaze shifts.

LARGE-AMPLITUDE GAZE SHIFTS. We first determined whether the dynamics of the vergence movements generated during combined eye-head gaze shifts were similar to those generated during head-restrained saccades. Figure 8 shows examples of 35° gaze shifts that contained a significant head contribution, and for which the peak conjugate *gaze* velocities and dynamics were matched to those of asymmetric head-restrained saccades with comparable amplitudes (compare with Fig. 6*B*). Interestingly, triphasic, oscillatory-like vergence movements were associated with each of these gaze shifts. Furthermore, these triphasic vergence movements were highly similar to those obtained during 35° saccades with comparable conjugate dynamics (compare the superimposed vergence velocity averages in the *inset* in Fig. 8). To complete this comparison, we plotted the relationships between the peak velocity of all three vergence phases and the peak conjugate *gaze* velocity (Fig. 7, *A–C*). The relationship between the peak velocity of each vergence phase and the peak conjugate gaze velocity was comparable for 35° gaze shifts (gray filled circles) and 35° asymmetric saccades (black filled squares). Similar trends were obtained for *monkey B* (see legend of Fig. 7). The relationship between the vergence dynamics and the gaze dynamics, not the eye dynamics (note the important differences between head-restrained and head-unrestrained eye movement dynamics, while vergence dynamics remain comparable), will be addressed in the DISCUSSION.

Figure 9 shows examples of 55° gaze shifts that had similar conjugate dynamics (i.e., oscillatory-like) to, and a longer duration than, 35° gaze shifts (240 ± 22 ms vs. 188 ± 14 ms, for 55 and 35° gaze shifts, respectively). As we predicted, these larger amplitude gaze shifts were accompanied by further unmasked oscillating vergence movements that consisted of *four* phases, i.e., divergence-convergence-divergence-*convergence*. Furthermore, as shown in Fig. 7, *A–C* (open diamonds), the relationship between the peak velocity of the first three vergence phases and the peak conjugate velocity of these large amplitude gaze shifts was comparable with that obtained for smaller amplitude saccades and gaze shifts with a terminal plateau. Finally, no significant relationship ($R = 0.24$, $P > 0.05$) was obtained between the peak velocity of the second convergent phase and the peak conjugate velocity of the gaze shifts. Similar results were obtained for *monkey B* (see legend of Fig. 7).

Timing of the vergence velocity profiles

The time course of the vergence velocity profiles that accompanied more symmetric bell-shaped saccades versus saccades/gaze shifts with more asymmetric velocity profiles can be directly compared in Fig. 10, *A* and *B* (*monkeys J* and *B*, respectively). Average vergence velocity profiles have been aligned relative to conjugate movement onset. For *monkey J*, the average traces represent the data illustrated in Figs. 1, 5, 6, 8, and 9. In addition, average vergence velocity profiles obtained for 45° gaze shifts are shown. The duration of the first divergent phase was remarkably constant across all saccades

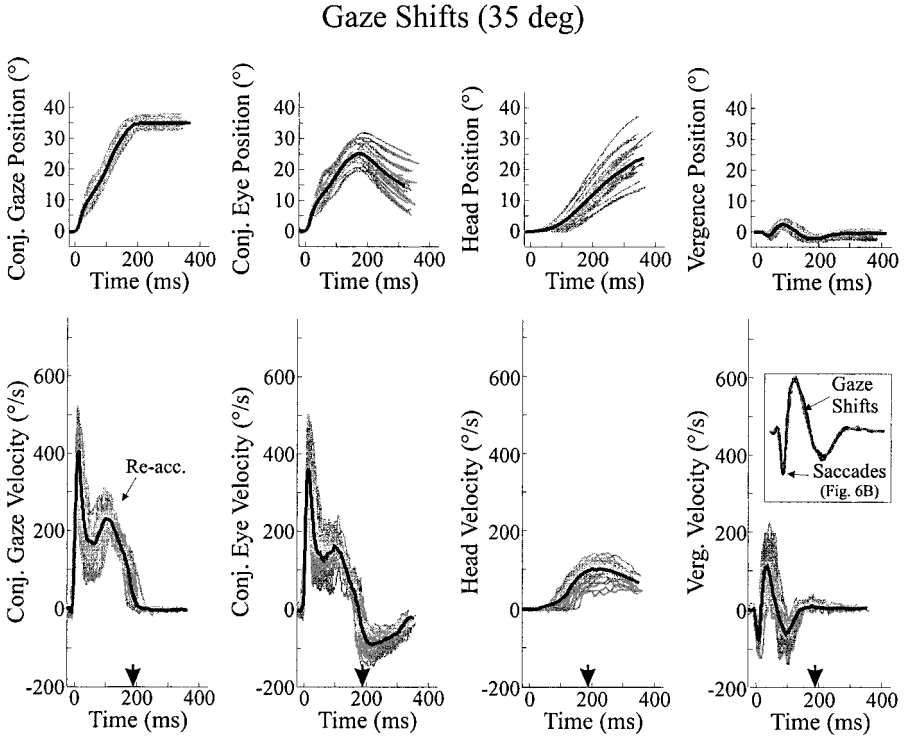

FIG. 8. Gaze shifts were accompanied by triphasic vergence movements. Individual (thin gray curves) and average (thicker black curves) conjugate gaze position, conjugate eye position, head position, and vergence position profiles for 35° combined eye-head gaze shifts ($n = 26$) are shown in the *top row* (*monkey J*), from *left* to *right*, respectively. The accompanying velocity profiles are shown in the *bottom row*. The filled arrows indicate the offset of the average conjugate gaze movement. A typical reacceleration similar to that of head-restrained saccades was clearly visible in the gaze conjugate velocity trace. *Inset*: superimposed average vergence velocity profiles associated with 35° gaze shifts (gray curve) and 35° saccades (black curve; from Fig. 6*B*) with comparable conjugate dynamics.

Downloaded from www.physiology.org/journal/jn at Johns Hopkins Univ Serials Dept Electronic (162.129.251.017) on July 26, 2019.

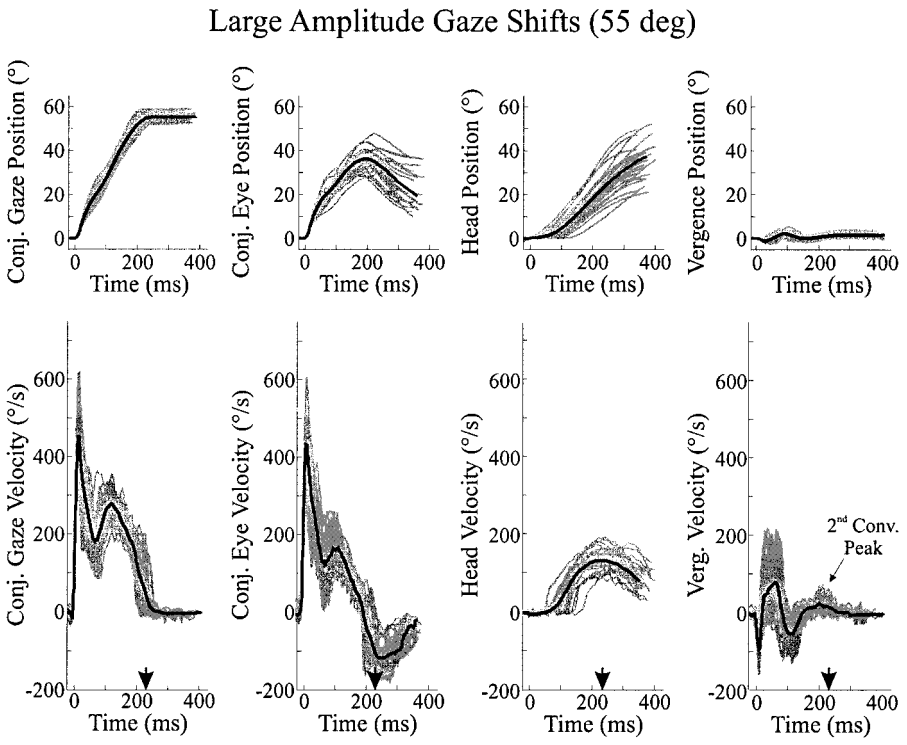

FIG. 9. Large-amplitude 55° gaze shifts were accompanied by a vergence velocity profile with a 2nd convergence phase for *monkey J* (2nd Conv. Peak; $n = 29$).

and gaze shifts (24 ± 9 and 29 ± 10 ms, *monkey J* and *B*, respectively) and was uncorrelated to the duration on the accompanying conjugate movement ($R = 0.41$ and 0.14, $P > 0.05$, *monkeys J* and *B*, respectively). On the other hand, the subsequent features of the vergence velocity trajectories varied across behaviors. During more symmetric saccades, the duration of the convergence phase of biphasic vergence transients was well correlated with the saccade duration ($R = 0.98$ and 0.92, $P < 0.05$, *monkeys J* and *B*, respectively). In contrast, during more asymmetric saccades and gaze shifts, the duration of the first convergence phase, as well as that of the second divergence and second convergence phase(s), were poorly or not correlated with the duration of the accompanying conjugate movement [$R = 0.17$, 0.22, and 0.62 (*monkey J*), and $R = 0.34$, 0.28, and 0.50 (*monkey B*), for the 1st convergence, 2nd divergence, and 2nd convergence phases, respectively]. In fact, the duration of these vergence phases remained relatively constant across all asymmetric saccades and gaze shifts, and also across the different vergence phases (mean duration = 67 ± 22 and 50 ± 19 ms, for *monkeys J* and *B*, respectively). Thus the latter portion of the vergence velocity trajectory oscillated at approximately 7.5 Hz for *monkey J* and 10 Hz for *monkey B*.

Furthermore, we found that on a trial-by-trial basis, the conjugate and vergence velocity profiles oscillated at comparable frequencies and were actually in phase with one another (Fig. 11, *A* and *B*, for saccades and gaze shifts, respectively). In general, the first divergence peak occurred concurrently with the initial peak conjugate velocity, and the second divergence phase occurred at the same time as the conjugate reacceleration peak. With respect to the first convergence phase, its peak velocity took place roughly half-way between the two conjugate peaks, which corresponds to the minimum conjugate velocity recorded in this interval. The second conjugate peak, when present, tended to arise simultaneously with small inflections in the conjugate profiles that followed the reacceleration peak.

Figure 12 further summarizes the relationship between the complexity of the vergence oscillations (i.e., the number of phases in the saccade/gaze shift-related vergence movements) and *1*) the dynamics of the gaze shift and *2*) the duration of the conjugate movement. For *monkey J*, saccades with more stereotyped bell-shaped dynamics, including those that had a mean duration exceeding 165 ms (i.e., the shortest mean conjugate duration associated with triphasic vergence movements), were always accompanied by a simple biphasic (divergence-convergence) vergence transient (Fig. 12*A*, open bars). In contrast, saccades and gaze shifts that had more asymmetric conjugate dynamics were accompanied by vergence velocity profiles that contained a second divergence and, sometimes, a second convergence phase (gray filled and black filled bars, for saccades with triphasic and quadriphasic vergence movements, respectively). For these movements, the total duration of the conjugate movement primarily determined the number of additional phases that were generated: saccades and gaze shifts with durations between 165 ± 16 and 188 ± 14 ms had only a second divergence phase, while larger gaze shifts with durations between 221 ± 8 and 240 ± 22 ms had both a second divergence phase and a second convergence phase. Figure 12*B* illustrates that very similar trends were also observed for *monkey B*. In general, the saccades and gaze shifts made by *monkey B* were faster than those made by *monkey J*, and consequently, the movement durations were shorter.

DISCUSSION

Experimental findings

In the present report, we have characterized the dynamic properties of the vergence movements that accompanied large-

Downloaded from www.physiology.org/journal/jn at Johns Hopkins Univ Serials Dept Electronic (162.129.251.017) on July 26, 2019.

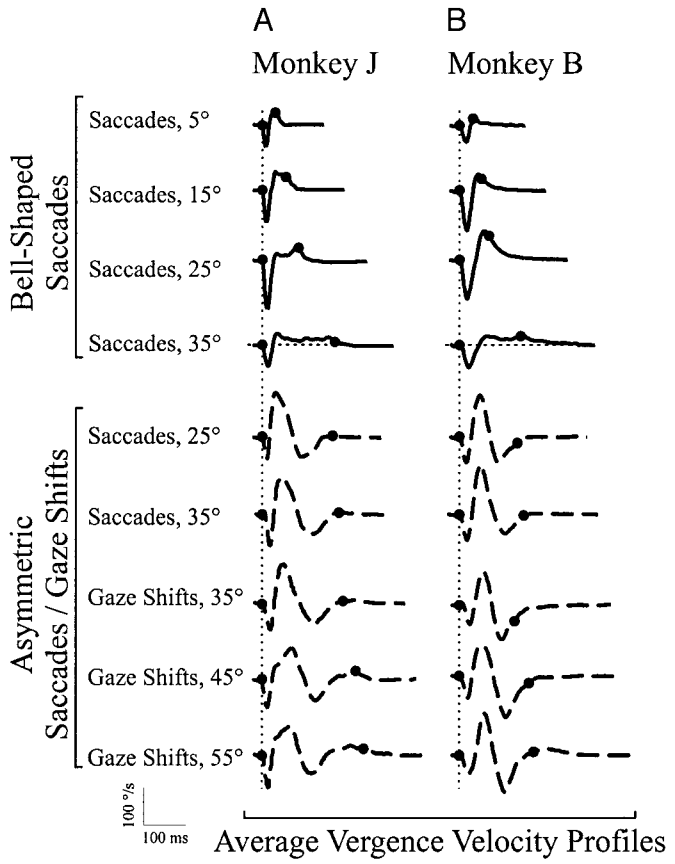

FIG. 10. Time course of the vergence velocity profiles that accompanied saccades and gaze shifts. Average vergence velocity profiles are shown for (*A*) *monkey J* and (*B*) *monkey B.* Note that for *monkey J*, the average traces represent the data previously illustrated in Figs. 1, 5, 6, 8, and 9. In addition, average vergence velocity profiles obtained for 45° gaze shifts are shown. The *top 4 traces* were associated with more symmetric saccades (5–35°), and the *bottom 5 traces* were associated with more asymmetric saccades (25–35°) and gaze shifts (35–55°). Average profiles were aligned on the onset of the conjugate movement (vertical dotted line, and leftmost dots). The offset of the average conjugate movement is also indicated for each trace (rightmost dots).

amplitude saccades with asymmetric, *oscillatory*-like dynamics (for examples of such movements, see Bahill and Stark 1975; Cullen and Guitton 1997a). Characteristically, these saccades had a reacceleration following the peak saccadic velocity. We also provided the first description of the vergence movements that accompanied eye-head gaze shifts, which as previously described, frequently have asymmetric dynamics (Cullen and Guitton 1997b; Cullen et al. 2000; Freedman and Sparks 1997; Phillips et al. 1995, 1999; Roy and Cullen 1998). All these rapid gaze movements, whether or not they were accompanied by head movement, had comparable dynamic vergence patterns. Furthermore, the observed vergence trajectories differed markedly from those that accompanied symmetric head-restrained saccades (Bruno et al. 1995; Collewijn et al. 1988, 1995, 1997; Eggert and Kapoula 1995; Erkelens et al. 1989; Fioravanti et al. 1995; Maxwell and King 1992; Oohira 1993; Zee et al. 1992). Instead of biphasic vergence transients, more complex *oscillatory*-like vergence patterns were unmasked. In the most extreme case, that is during large amplitude (55°) combined eye-head gaze shifts, a divergence that was followed by a convergence phase, a second divergence and a second convergence phase was observed (see Fig. 9). These vergence movements oscillated at a constant frequency for a given animal (7.5–10 Hz), and in phase with the conjugate movements.

In agreement with previous studies (Bruno et al. 1995; Collewijn et al. 1988, 1995, 1997; Eggert and Kapoula 1995; Erkelens et al. 1989; Fioravanti et al. 1995; Maxwell and King 1992; Oohira 1993; Zee et al. 1992), we also observed highly stereotyped biphasic vergence velocity profiles (i.e., divergence-converge) during saccades with more *symmetric* (more bell-shaped) conjugate velocity profiles. Similarly, the relationships we measured between the peak velocity of the saccades and both the peak divergence and convergence velocities of the transients were quantitatively comparable to those previously reported in monkeys (Maxwell and King 1992). We also extended the findings of these previous studies and showed that the metrics of biphasic vergence transients depend on the presaccadic eye position; the divergence and convergence peak velocities were faster for saccades of a given amplitude and direction that originated from an eccentric position and ended at the primary position (i.e., centripetal) versus those that originated from the primary position and ended at an eccentric position (i.e., centrifugal). We found that this effect could be accounted for by the previously documented faster peak conjugate velocities of centripetal saccades (Collewijn et al. 1988). Finally, in agreement with results for humans (Collewijn et al. 1995, 1997), we observed that the duration of the biphasic

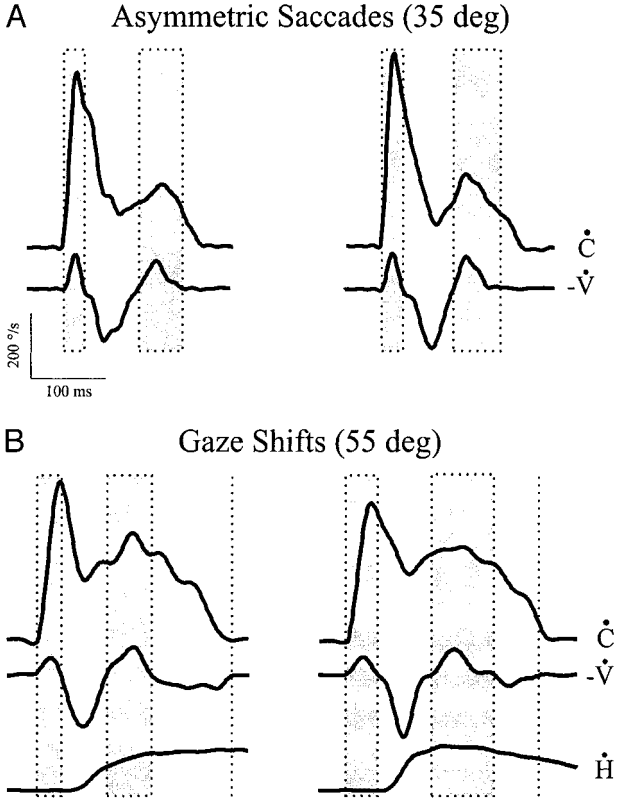

FIG. 11. Good temporal alignment was observed between the oscillation phases of the conjugate and vergence velocity profiles during asymmetric saccades and gaze shifts. *A*: 2 examples of asymmetric 35° saccades. The vergence velocity trace was inverted to facilitate the comparison. Gray shaded boxes are aligned on the beginning of the 1st and 3rd phases of the vergence oscillation, and their width corresponds to the respective phase durations. *B*: 2 examples of more asymmetric, larger amplitude (55°) gaze shifts. The vertical dotted lines represent the end of the 4th vergence oscillation phase.

Downloaded from www.physiology.org/journal/jn at Johns Hopkins Univ Serials Dept Electronic (162.129.251.017) on July 26, 2019.

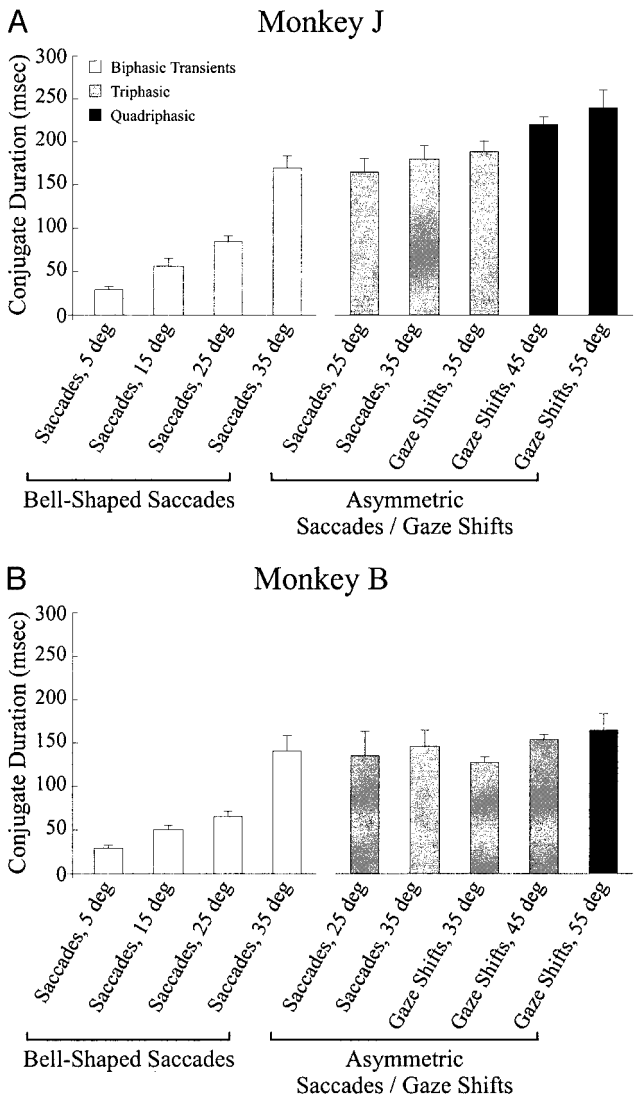

FIG. 12. Summary of the relationship between the number of phases in the saccade/gaze shift-related vergence movements and the dynamics and duration of the associated conjugate movements. Data for *monkeys J* and *B* are shown in *A* and *B*, respectively. The height of the bars represents the mean duration of the conjugate movements (±SD). Open bars represent biphasic vergence velocity profiles, gray filled bars represent triphasic vergence velocity profiles, and black filled bars represent quadriphasic vergence velocity profiles.

vergence transients increased with the amplitude/duration of small symmetric saccades. The increase in duration was primarily due to the temporal stretching of the convergence component, since the duration of the initial divergence component remained roughly constant.

Peripheral mechanisms and vergence oscillations

Previous modeling efforts have shown that peripheral mechanisms can generate the biphasic vergence transients associated with symmetric saccades (Zee et al. 1992). To investigate whether this model could reproduce the complex vergence movements associated with more asymmetric saccades, we implemented a computer simulation based on the original model of Zee et al. (1992). In agreement with Zee and colleagues, we found that *1*) mechanical asymmetries in the abducting/adducting eye plant dynamics (i.e., different time constants), *2*) differences in premotor delays due to the additional synapse in the medial rectus subdivision of the oculomotor nuclei, or *3*) a combination of both mechanisms, were sufficient to account for the biphasic vergence velocity profiles observed during symmetric saccades (Fig. 13*A*). Then, to pro-

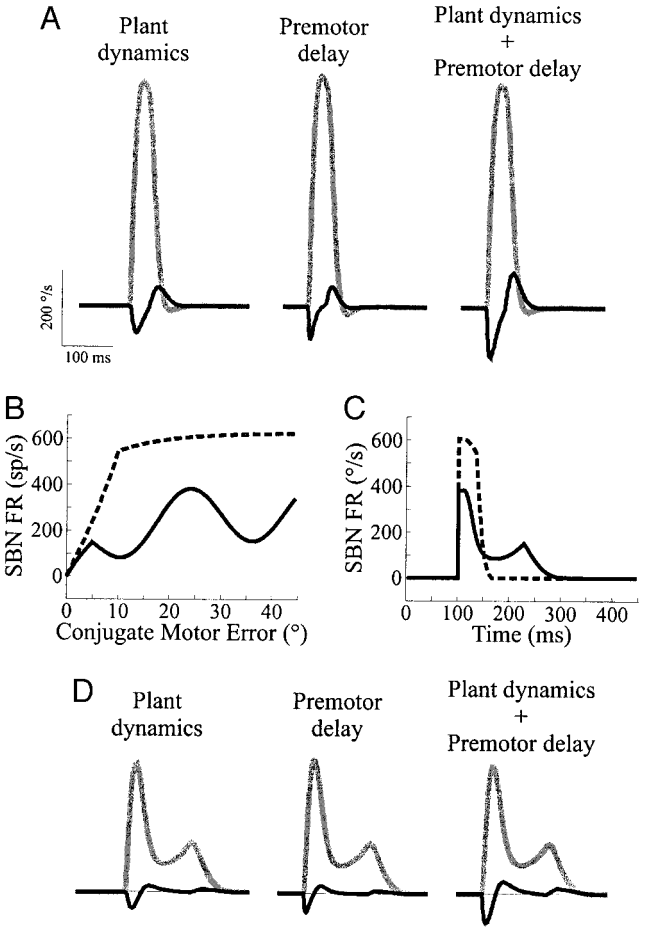

FIG. 13. Computer simulations of vergence transients based on peripheral mechanisms alone. The model structure is as described in Zee et al. (1992). *A*: simulated conjugate (gray curve) and vergence (black curve) velocity profiles for more symmetric 25° saccades. The *asymmetries in plant dynamics* (13- vs. 10-ms time constants, abducting and adducting muscles, respectively) and the *premotor delay* (additional 1.9-ms delay to adducting muscle) models, as well as a model that combined the 2 mechanisms, yielded biphasic vergence transients. Note that the maximum firing rate values that could be reached by saccadic burst neurons (SBN) were raised from 400–440 spikes/s to 600–640 spikes/s (AR and AL in the SBN nonlinearity function, respectively) to account for the faster saccades made by monkeys. *B*: nonlinear functions describing the saccadic burst neurons (SBN) discharge, FR(t), as a function of the instantaneous conjugate motor error, cme(t), for more symmetric saccades (dashed curve), and more asymmetric saccades (solid curve). The function for more symmetric saccades was as described in Zee et al. (1992). To generate more asymmetric saccades, the nonlinear function described in Zee et al. (1992) was scaled down to 65% of its amplitude, and the resulting curve was convolved with a sine wave function of the instantaneous conjugate motor error ($S = A \sin [2\pi\omega * cme(t) + \phi]$, where $A = 120$ spikes/s, $\omega = 0.04$ rad/s, and $\phi = 4/7\pi$ rad). *C*: simulated SBN discharges during more symmetric (dashed curve) and more asymmetric (solid curve) 25° saccades, as obtained with the functions described in *C*. The accompanying conjugate velocity profiles are shown in *A* and *D*, respectively. *D*: conjugate (gray curve) and vergence (black curve) velocity profiles for more asymmetric 25° saccades. Note that the characteristic reacceleration phase associated with more asymmetric saccades was reproduced in the simulations. Triphasic vergence velocity profiles were clearly elicited by these modified models. However, a divergence-convergence-*convergence* pattern was consistently observed, which differs from our experimental observations (divergence-convergence-divergence).

Downloaded from www.physiology.org/journal/jn at Johns Hopkins Univ Serials Dept Electronic (162.129.251.017) on July 26, 2019.

duce saccades with more asymmetric dynamics, we altered the model's relationship between the conjugate motor error and the saccadic burst neuron firing rate (Fig. 13*B*, solid curve) (see Figs. 11 and 19 in Zee et al. 1992). This modification resulted in a "reacceleration" phase in the burst neuron discharge (Fig. 13*C*, solid curve), which in turn produced conjugate movements with more asymmetric dynamics that were comparable to our experimental observations (Fig. 13*D*, dotted curve). The modification was placed at the level of the saccadic burst neurons given that asymmetries have been reported in the discharges of inhibitory burst neurons during saccades and gaze shifts with reacceleration phases (Cullen and Guitton 1997a,b). With this modification, the model clearly yielded triphasic vergence movements. However, the pattern of vergence movements was a divergence component followed by two separate convergence components, and therefore differed from the divergence-convergence-*divergence* pattern that we observed experimentally (compare Fig. 13*D* with Fig. 5*B*). Doubling or halving the values of the extraocular muscle time constants and/or the value of the relative motor delays to each eye had no effect on the pattern described above. Thus the peripheral mechanisms tested could not reproduce the oscillatory-like patterns observed experimentally. We propose that a yet unidentified mechanism(s) is recruited or unmasked during asymmetric conjugate movements to complement the peripheral mechanisms, and suggest that the oscillatory-like nature of the complex vergence and conjugate movements indicates that this additional mechanism(s) is centrally based.

Central mechanisms and vergence oscillations

Classically, models for the control of three-dimensional binocular eye movements have employed separate controllers to drive the conjugate and the vergence components of movements (see Mays 1998). However, a number of recent studies have provided evidence that the neural substrate for disjunctive saccades is a more *integrated* mechanism in which a shared controller drives both the conjugate and the vergence components of eye movements. Indeed, the saccadic burst generator, which had commonly been assumed to encode purely conjugate movements (reviewed in Mays and Gamlin 1995a), is likely to carry a shared signal that encodes vergence as well as conjugate information during disjunctive saccades. For example, electrical stimulation of the caudal region of the superior colliculus perturbs both components of disjunctive saccades (Chaturvedi and Van Gisbergen 1999). Brain stem saccadic burst neurons, which are driven by the output neurons of the caudal superior colliculus, preferentially encode the monocular movement of the ipsilateral or contralateral eye (where monocular eye position = conjugate position ± ½ * vergence position) rather than the conjugate eye movement (Sylvestre and Cullen 1999b; Zhou and King 1998). Moreover, both the vergence and the conjugate components of disjunctive saccades can be slowed down by electrical stimulation of neurons in the rostral region of the superior colliculus (Chaturvedi and Van Gisbergen 2000), and their brain stem target (the omnipause neurons of the nucleus raphe interpositus) (Mays and Gamlin 1995a,b). On the one hand, given that omnipause neurons directly inhibit brain stem saccadic burst neurons (Curthoys et al. 1984; Strassman et al. 1987), which encode vergence as well as conjugate eye movements, the effect of stimulation may be mediated, at least in part, by inhibition of the saccadic burst generator. On the other hand, it has been proposed (Chaturvedi and Van Gisbergen 2000; Mays and Gamlin 1995a,b) that the effect of stimulation on vergence eye movements results from omnipause neuron inhibition of a distinct population of neurons, termed vergence velocity neurons (Mays and Gamlin 1995a). These neurons have been shown to discharge vigorously during disjunctive saccades (when omnipause neurons cease firing) and remain silent during conjugate saccades (Mays and Gamlin 1995b). In fact, the most likely scenario, which incorporates all available neurophysiological data, is that disjunctive saccades are driven by the superior colliculus via *both* the brain stem saccadic burst neurons and the midbrain vergence burst neurons, and that the inhibition of both neuron types via omnipause neurons slows the vergence as well as the conjugate components of the movement.

Further support for an integrated mechanism for the control of conjugate and vergence movements during saccades comes from our observation that the oscillations in the conjugate and vergence velocity profiles were temporally well correlated (see Fig. 11). It is unlikely that two independent central mechanisms with no interconnections would produce synchronized oscillatory conjugate and vergence movements during saccades. It is even more unlikely, if not impossible, that two independent mechanisms would remain robustly synchronized across gaze shifts of different amplitudes and durations made with or without head movements. We therefore propose that the comparable oscillatory dynamics of the conjugate and the vergence movements must result from a shared drive. In the following sections, we will further this proposal by addressing two questions: first, how are the oscillations generated; and second, what underlies the coupling between the oscillations observed on conjugate and vergence movements?

Model simulations: conjugate oscillations

To determine the mechanism(s) underlying the conjugate oscillations described in the present report, we utilized computer simulations of a previously published model of gaze control (Galiana and Guitton 1992). This model integrates eye and head control by placing the superior colliculus inside a premotor feedback loop and uses its "alertness" level to modulate the speed of gaze shifts. A number of subsequent experiments supported these model assumptions: *1*) the superior colliculus is located within the feedback circuit that controls saccade execution (see review by Sparks 1999), *2*) increased target uncertainty (e.g., Basso and Wurtz 1997) and/or decreased attention (e.g., Munoz et al. 1991) modulate the level of activity of collicular neurons, and *3*) lower activity of collicular neurons has been associated with slower and more variable gaze shift dynamics (e.g., Du Lac and Knudsen 1990; Freedman et al. 1996; Munoz et al. 1991). Here we argue that variations in the monkey's behavioral state could render the collicular feedback loop more prone to oscillations.

More specifically, we propose a mechanism in which the net feedback loop delay would vary as a function of the animal's behavioral state (see diagram in Fig. 14*A*). As a result, behavioral conditions that cause larger delays and/or larger premotor recruitment levels would cause oscillations in the conjugate profiles of saccades, whether the head is restrained or unre-

Downloaded from www.physiology.org/journal/jn at Johns Hopkins Univ Serials Dept Electronic (162.129.251.017) on July 26, 2019.

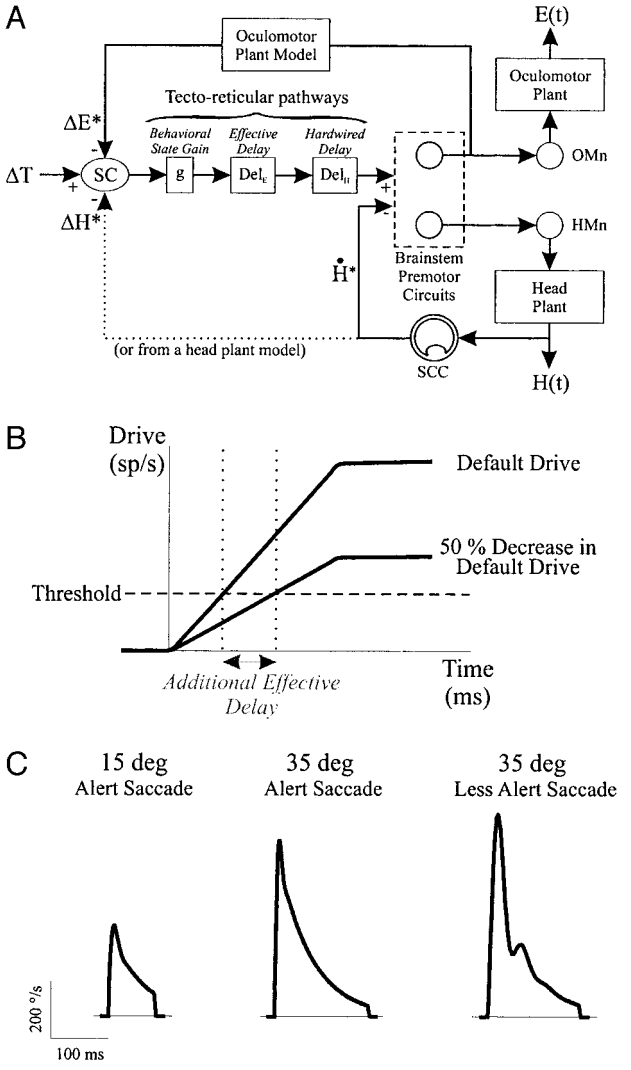

FIG. 14. Computer simulations of conjugate oscillations. *A*: schematic of the model utilized for the simulations. For the sake of simplicity, this model only generates conjugate eye movements. Note, however, that in the bilateral version of this model (Cova and Galiana 1995, 1996), the integrated conjugate/vergence controller would assure that dynamics present on the conjugate movements (e.g., oscillations) would automatically appear on the vergence movements (see APPENDIX). The eye plant is represented with 2nd-order dynamics and a slide term [plant $\rightarrow (cs + 1)/(us^2 + rs + k)$; $c = 0.06$, $u = 0.002$, $r = 0.5$, $k = 4$ (from Sylvestre and Cullen 1999a)]. A net functional delay varies with behavioral state (see text for details). To simulate head-unrestrained gaze movements, the eye and head premotor circuitries receive a gaze-related input from a shared upstream gaze-based controller, and therefore the eye and head trajectories are not independent. ΔT, desired change in gaze position; ΔE^*, ΔH^* and $\dot{H}^*$, efference copy of current eye displacement, head displacement, and head velocity, respectively; $E(t)$ and $H(t)$, actual eye and head position, respectively; OMn and HMn, extraocular and head motoneurons, respectively; SCC, semicircular canals. *B*: illustration of the impact of decreasing the "behavioral state gain" on the value of the effective delay. *C*: simulated conjugate velocity profile during small 15° saccade and "normal" alertness level [*leftmost panel;* $g = 40$, total delay (i.e., $\text{Del}_E + \text{Del}_H$) = 5 ms], during 35° saccade and "normal" alertness level (*middle panel;* $g = 70$, total delay = 3 ms), and during the same 35° saccades and decreased level of alertness (*rightmost panel;* $g = 35$, total delay = 9 ms). Note the characteristic oscillatory-like pattern in the last case.

strained. Two simple extensions from the Galiana-Guitton model (1992) are included: the tecto-reticular pathway now has a delay element that has been broken down into a fixed component and a variable component, and the eye plant is now more accurately represented as second-order with a slide term in the numerator of its transfer function (see legend of Fig. 14). First, the fixed delay component is represented in Fig. 14*A* by the *hardwired delay*, and it corresponds to the minimum possible delay, under optimal conditions, from superior colliculus modulation to changes in eye movements. As an estimate for this value, we utilized the difference between the latency of electrical perturbations during ongoing large amplitude saccades (10–11 ms) (Munoz et al. 1991) and the expected abducens lead time during saccades (in the order of 9 ms) (Sylvestre and Cullen 1999a). Hence the minimal collicular-brain stem delay was set to 1–2 ms. Second, the variable *effective delay* represents the postulated effect of the monkey's behavioral state on downstream recruitment and transmission delays. As is illustrated in Fig. 14*B*, lowering the value of the behavioral gain element could increase this functional delay by lengthening the time period necessary to reach a recruitment threshold. In agreement with this proposed mechanism, microstimulation studies in the superior colliculus (Freedman et al. 1996; Munoz et al. 1991) have shown that low-frequency stimulation trains tend to generate gaze shift with more variable latencies and often oscillating dynamics comparable with those reported here (e.g., Fig. 5 in Freedman et al. 1996). Also consistent with this mechanism is the finding by Bahill and Stark (1975) that low-frequency, long-duration, non–main sequence saccades are always observed when subjects are fatigued. Indeed, in the present study, we noted that slower saccades with conjugate oscillations tended to be more frequent toward the end of experimental sessions when the animal was presumably more tired and less attentive: for saccades larger than 25°, the ratio of asymmetric to symmetric saccades roughly doubled during the last 10 min versus the first 10 min of an experiment, reaching values up to approximately 20%.

Simulations of the extended Galiana-Guitton model demonstrated that by simply increasing the feedback loop effective delay (from realistic 3 to 9 ms) and reducing the behavioral gain, oscillatory conjugate movements could be generated. With a high behavioral state gain and small delays, the model yielded smooth and fairly symmetric conjugate velocity profiles for small amplitude saccades (Fig. 14*C*, *leftmost panel;* compare with Fig. 1*B*), while more asymmetric, yet not oscillating, conjugate velocity profiles were obtained for larger amplitude saccades (Fig. 14*C*, *middle panel;* compare with Fig. 6*A*). On the other hand, when the behavioral state gain was decreased by 50% (e.g., decreased alertness) and the effective delay was consequently increased, conjugate oscillations could be readily generated (Fig. 14*C*, *rightmost panel;* compare with Fig. 6*B*). We conclude that context-dependent delays in the superior colliculus–brain stem premotor loops are a likely source for the conjugate oscillations described in the present report.

Coupling of conjugate and vergence oscillations

As was described above, there is considerable experimental evidence suggesting that the control of conjugate and vergence movements, at least during saccades, is integrated within a shared controller. Because the Galiana-Guitton model, like most published models of gaze control, was designed to produce conjugate gaze movements only, we could not directly

Downloaded from www.physiology.org/journal/jn at Johns Hopkins Univ Serials Dept Electronic (162.129.251.017) on July 26, 2019.

simulate the coupling of conjugate and vergence oscillations. However, based on anatomy and our current binocular control models (Cova and Galiana 1995, 1996), it is expected that any conjugate oscillations would be accompanied by vergence oscillations, even with a purely conjugate task. This is further developed in the APPENDIX with a simple example.

Vergence oscillations during gaze shifts

Our head-unrestrained analysis revealed that the properties of the conjugate and vergence oscillations during combined eye-head gaze shifts were related to the *gaze* movements in a similar manner as during head-restrained saccades (e.g., Fig. 11). This was most evident toward the end of gaze shifts: although the eyes actually reversed direction, the gaze conjugate and vergence velocity profiles did not differ markedly from those recorded during saccades of comparable gaze amplitudes and dynamics (see the *inset* in Fig. 8). Such a relationship between vergence dynamics and gaze rather than eye movements may appear surprising given that vergence movements are usually considered as purely oculomotor events. However, this apparent discrepancy may be better understood if one considers the following. There is accumulating evidence that the superior colliculus generates a signal for the desired gaze displacement during gaze shifts that in turn drives eye and head premotor pathways (reviewed in Galiana and Guitton 1992; Sparks 1999). Given our postulate that the superior colliculus is the central source of the conjugate and vergence oscillations, it then follows that these oscillations should be better correlated with the gaze than with the eye velocity profiles. Our results therefore provide indirect evidence that gaze shifts are controlled by a common gaze-based controller.

General conclusions

In summary, we show that *1*) the presaccadic eye position affects the biphasic vergence transients that accompany more symmetric saccades in a manner that is predictable based on differences in saccadic speeds; *2*) conjugate velocity profiles that exhibit oscillatory-like properties are accompanied by vergence velocity profiles that also oscillate; *3*) for these movements, conjugate and vergence velocity profiles oscillate together at a fixed frequency; *4*) combined eye-head gaze shifts exhibit conjugate gaze and vergence oscillations that are highly comparable with those of head-restrained saccades; and *5*) peripherally based models for the generation of biphasic vergence transients cannot account for the oscillatory behavior described in the present report. We conclude that the results presented in this report provide strong evidence that conjugate and vergence movements are generated by a shared central mechanism that effectively functions as a binocular gaze controller.

APPENDIX

In this paper, a model of conjugate saccades and gaze shifts was used to illustrate how central delays and gains on tecto-reticular projections could be responsible for oscillatory conjugate responses in iso-vergence tasks. This model (Fig. 14*A*) is a simplified form of a bilateral binocular control circuit proposed by Cova and Galiana (1995, 1996), which has been previously shown to produce realistic conjugate vestibuloocular reflex, slow-phase vergence tracking movements, and vergence nystagmus (Cova and Galiana 1994). Subsequent extensions of this model support its compatibility with observed neurophysiology on several vestibular nuclei (VN) premotor cell types (Green and Galiana 1996). Anatomical and physiological support for the structural elements of these models can be found in those references. The main point is that binocular (disconjugate) control can arise from a single shared bilateral controller. Hence any dynamics (including oscillations) in the conjugate trajectories of ocular responses are expected to also be reflected in the vergence traces, when present.

Model description

First let us review in more detail the form of the model used to simulate conjugate eye movements. The schema shown in Fig. A1*A* is equivalent to that shown in Fig. 14*A*, with the exception that the head controller has been removed and that the brain stem premotor circuits (dotted box in Fig. 14*A*) have now been explicitly defined. The main points of interest are that gaze error signals from the superior colliculus (SC) project both to the contralateral long lead burst neurons (LLBN) and to the contralateral vestibular nucleus–nucleus prepositus hypoglossi complex (VN-PH), and that the eye plant (conjugate) receives the same premotor drives as the VN-PH complex. This collapsed form of premotor signals represents the net contribution of neurons on both sides of the brain stem to the conjugate eye movements. For rightward conjugate saccades, excitatory burst neurons (EBNs) are active only on the right side of the brain stem, the output of the VN-PH complex is the net difference between left and right premotor drives, and the conjugate efference copy is related to the difference between the right and left "tonic" VN-PH signals. However, this type of diagram carries with it the false impression that vergence must arise from a separate premotor system.

Figure A1*B* describes the main anatomical pathways involved in binocular saccades. Several known pathways (such as direct SC connections to motoneurons) have been omitted for simplicity without altering the arguments that follow. In this anatomically based model, it is presumed that *1*) all premotor signals projecting to motoneurons also project to a PH (Cova and Galiana 1995, 1996); *2*) each PH processes signals in a manner analogous to the eye plants to produce accurate *monocular* efference copies (Cova and Galiana 1995, 1996; supported by neurophysiological data from King et al. 1994; McConville et al. 1994; Zhou and King 1996); *3*) the VN, PH, and SC are tightly interconnected during the execution of saccades (e.g., Cova and Galiana 1995, 1996); and *4*) brain stem premotor activity is better related to *monocular* eye positions than to conjugate eye positions (Cova and Galiana 1995, 1996; see review of neurophysiological evidence in King and Zhou 2000). In the diagram of Fig. A1*B*, neurons labeled in dark fonts are activated during rightward conjugate eye movements, while those labeled in gray either decrease their activity or are not modulated during the same movements. Note that the opposite pattern would occur for leftward saccades (i.e., gray-labeled neurons would be activated and black-labeled neurons would be inhibited). However, with respect to binocular control, it is more appropriate to associate increased activity in black-labeled neurons with *temporal* movements of the right eye (or decreased activity in gray-labeled neurons with nasal movements of the left eye).

In this bilateral connectivity, and assuming the efference copies are accurate and increasing with monocular *temporal* movements, one can define

$$\text{efference vergence command} \rightarrow -[E_R^* + E_L^*]\text{; positive for convergence}$$

$$\text{efference conjugate command} \rightarrow [E_R^* + E_L^*]/2\text{; positive for rightward} \quad (A1)$$

The efference copies on each side (E_R^* and E_L^* on the right and left sides, respectively) here code for ipsilaterally directed eye position. Behavioral conjugate and vergence movements are defined in exactly the same way as *Eq. A1*.

Downloaded from www.physiology.org/journal/jn at Johns Hopkins Univ Serials Dept Electronic (162.129.251.017) on July 26, 2019.

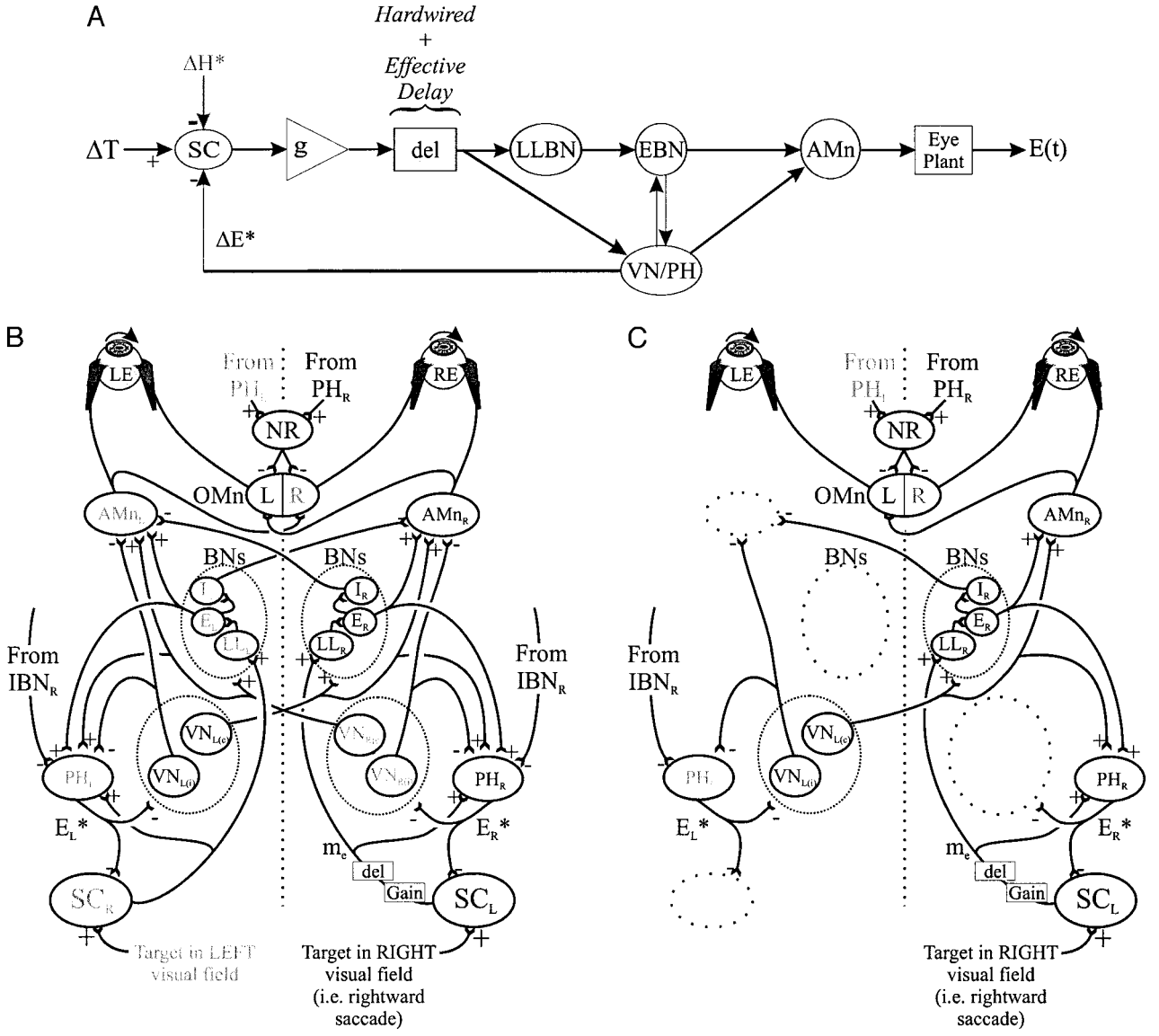

FIG. A1. *A*: block diagram of the model used to simulate conjugate eye movements. This schema is equivalent to that shown in Fig. 14*A*, with the exception that the premotor structures (dotted box in Fig. 14*A*) are now shown. *B*: main bilateral anatomical pathways for saccadic control with collicular projections in the brain stem. The superior colliculi (SC) were transposed to simplify the diagram. Note the pronounced anatomical symmetry. The vertical dotted line denotes the midline. Neurons labeled in dark fonts increase their activity during rightward conjugate eye movements, while those labeled in gray either decrease their activity or are not modulated. Uppercase subscripts indicate that a neuron is located on the left or right side of the brain stem, and when present, lowercase subscripts in parentheses refer to the projection side of the neuron type (i.e., ipsilaterally or contralaterally). LE and RE, left and right eyes, respectively; NR, near response cells; OMn, oculomotor nucleus; AMn, abducens nucleus; BNs, burst neurons (E, excitatory; I, inhibitory; LL, long lead); VN, vestibular nuclei neurons; PH, nucleus prepositus hypoglossi neurons; SC, superior colliculus neurons; E*, efference copy; m_e, motor error; del, net feedback loop delay; Gain, output gain of the SC. *C*: reduced active pathways from *B*, when a large-amplitude saccade is oriented to a far target to the right. In this case, premotor signals are controlled by the left superior colliculus, left VN, both PHs, and right bursters; neurons in the right superior colliculus, premotor VN cells on the right, burst neurons on the left, and abducens neurons on the left are presumed silenced. Note that the functional anatomy is no longer symmetric.

Sources of vergence transients during conjugate saccades

During small-amplitude rightward saccades that are purely conjugate as expressed on efference copies, the PH activity on both sides should be reciprocal. This is especially likely to be true for rightward saccades starting leftward of the primary position, for which the VN cells ipsilateral to the saccade are pausing, and those on the contralateral side may also pause because of their reduced tonic component. In this case, the premotor drive to PHs on both sides are dominated by burst projections and are more likely to produce symmetrically modulated efference copies ($E_R^* = -E_L^*$). Hence, during these movements, inputs onto the near response cells (NR), which are thought to drive vergence movements (Mays 1984; Mays and Gamlin 1995a,b; Mays et al. 1986) and have been postulated to originate in both PHs (Cova and Galiana 1995, 1996; King and Zhou 2000), will cancel out (see Fig. A1*B*) such that there will be no specific vergence-related drive to the oculomotor nucleus (OMn). Despite this, there is still potential for a small transient vergence component at the behavioral level since the anatomical projections to the abducens and oculomotor nuclei differ (Grantyn et al. 1980). Hence, during a conjugate saccade, it is possible

Downloaded from www.physiology.org/journal/jn at Johns Hopkins Univ Serials Dept Electronic (162.129.251.017) on July 26, 2019.

the excitatory and/or inhibitory drives to the abducens nucleus (AMn) and OMn are not perfectly matched; any differences in the agonist/antagonist drives to the left and right eyes would result in vergence movements.

In the more general case, however, and especially for larger amplitude saccades to far eccentric targets on the same side as the saccade direction (i.e., right of the primary position for rightward saccades), the functional anatomy for a conjugate goal is not symmetric (Fig. A1*C*). In the case of a large-amplitude rightward saccade, *1*) only the left SC, which projects to the PH (Grantyn and Grantyn 1982; Magnin et al. 1983) and long lead burst neurons (LLBNs) on the right (Keller et al. 2000), are active; *2*) EBNs excite AMn on the right side, and inhibitory burst neurons (IBNs) silence the left AMn; a nonreciprocal effect (Strassman et al. 1986a,b); *3*) EBN and IBN do not have identical firing profiles (Phillips et al. 2001), and so the effects on efference copies will be nonreciprocal; and *4*) there may be residual activity on the premotor VN cells contralateral to saccade direction since the saccade is in the ON-direction of their tonic component, but the ipsilateral VN cells usually pause (Cullen and McCrea 1993; Scudder and Fuchs 1992).

Thus in this model, there are two levels of interactions that can cause vergence components in binocular saccades to isovergence targets. At the *motor level*, the antagonist motor nuclei are not necessarily matched in discharge profiles, and so it is possible for both eyes to have different antagonist muscle activity (e.g., right medial rectus and left lateral rectus) despite possibly identical agonist activity (e.g., right lateral rectus and left medial rectus, via abducens internuclear neurons). At the *central level*, any mismatch in drives generating the monocular efference copies will permit the vergence content at premotor levels ($-[E^*_R + E^*_L]$) to affect OMn bilaterally via NR cells.

In summary, for small-amplitude saccades, the biphasic vergence transients probably reflect a simple mismatch in the AMn-OMn drives to each eye (i.e., motor level), while more severe forms of unwanted vergence such as those encountered during larger amplitude saccades could be due to additional mismatch in efference copies because of nonsymmetrical premotor signals, producing an erroneous vergence drive on NR/OMn (i.e., central level).

Vergence oscillations

In Fig. A1*C*, the case of a large-amplitude rightward saccade made to a far isovergence target is described. Clearly, this structure "folded" along the midline resembles the model for conjugate saccades shown in Fig. A1*A*. However, it is now obvious that the binocular controller during saccades (i.e., the left and right PHs) is strongly coupled by premotor loops through the burst neurons (BNs) and directly through the SC. As a result, premotor signals and their dynamics must be shared by both conjugate and vergence trajectories, whether at behavioral or efference copy levels. If the loop dynamics become oscillatory because of changes in arousal (as postulated in this paper), then oscillations will appear synchronized on both vergence and conjugate components.

The qualitative arguments above can be quantified with simple equations. Referring to Fig. A1*C*, for a rightward conjugate saccade

$$E^*_R = [m_e + VN_{L(c)} + EBN_R]P(s)$$

$$E^*_L = -[VN_{L(i)} + IBN_R]P(s) \quad (A2)$$

where P(s) represents the filter dynamics in each PH and are assumed to be similar to the eye plant dynamics, and the other variables represent activity on premotor cell types. By substitution into *Eq. A1*

$$\text{vergence } \alpha - [m_e + (VN_{L(c)} - VN_{L(i)}) + (EBN_R - IBN_R)]P(s) \quad (A3a)$$

$$\text{conjugate } \alpha \tfrac{1}{2}[m_e + (VN_{L(c)} + VN_{L(i)}) + (EBN_R + IBN_R)]P(s) \quad (A3b)$$

where *Eq. A3b* corresponds to the signal represented in the conjugate model described in DISCUSSION. As can be seen from *Eqs. A3a* and *A3b*, the conjugate and vergence signals are weighted sums of the same central signals, and unless bilateral modulations are truly reciprocal (i.e., differences = 0), some vergence signal will always be associated with a conjugate signal. Furthermore, all central activities, and hence conjugate and vergence signals, will share the dynamics of the network (i.e., the equation poles), so that conjugate oscillations will always be accompanied by vergence oscillations. Hence, despite a purely conjugate target, binocular saccades in the model can be disconjugate and oscillatory, depending on pathway parameters.

The authors thank J. E. Roy and M. Huterer for critically reading the manuscript. We also thank E. Moreau, W. Kucharski, J. Knowles, and A. Smith for outstanding technical assistance.

This study was supported by the Canadian Institutes of Health Research, the Natural Science and Engineering Research Council of Canada, and the Fonds de la Recherche en Santé du Québec.

REFERENCES

BAHILL AT AND STARK L. Overlapping saccades and glissades are produces by fatigue in the saccadic eye movement system. *Exp Neurol* 48: 95–106, 1975.

BASSO MA AND WURTZ RH. Modulation of neural activity by target uncertainty. *Nature* 389: 66–69, 1997.

BRUNO P, INCHINGOLO P, AND VAN DER STEEN J. Unequal saccades produced by aniseikonic patterns: a model approach. *Vision Res* 35: 3473–3492, 1995.

CHATURVEDI V AND VAN GISBERGEN JAM. Perturbation of combined saccade-vergence movements by microstimulation in monkey superior colliculus. *J Neurophysiol* 81: 2279–2296, 1999.

CHATURVEDI V AND VAN GISBERGEN JAM. Stimulation in the rostral pole of monkey superior colliculus: effects on vergence eye movements. *Exp Brain Res* 132: 72–78, 2000.

COLLEWIJN H, ERKELENS CJ, AND STEINMAN RM. Binocular co-ordination of human horizontal saccadic eye movements. *J Physiol (Lond)* 404: 157–182, 1988.

COLLEWIJN H, ERKELENS CJ, AND STEINMAN RM. Voluntary binocular gaze-shifts in the plane of regard: dynamics of version and vergence. *Vision Res* 35: 3335–3358, 1995.

COLLEWIJN H, ERKELENS CJ, AND STEINMAN RM. Trajectories of the human binocular fixation point during conjugate and non-conjugate gaze-shifts. *Vision Res* 37: 1049–1069, 1997.

COVA A AND GALIANA HL. Providing distinct vergence and version dynamics in a bilateral oculomotor network. *Vision Res* 35: 3359–3371, 1995.

COVA A AND GALIANA HL. A bilateral model integrating vergence and the vestibulo-ocular reflex. *Exp Brain Res* 107: 435–452, 1996.

COVA AC AND GALIANA HL. A bilateral model of vergence nystagmus. *Proc 16th IEEE EMBS, Baltimore, MD,* November 3–6, p. 263–264, 1994.

CULLEN KE, GALIANA HL, AND SYLVESTRE PA. Comparing extraocular motoneuron discharges during head-restrained saccades and head-unrestrained gaze shifts. *J Neurophysiol* 83: 630–637, 2000.

CULLEN KE AND GUITTON D. Analysis of primate IBN spike trains using system identification techniques. I. Relationship to eye movement dynamics during head-fixed saccades. *J Neurophysiol* 78: 3259–3282, 1997a.

CULLEN KE AND GUITTON D. Analysis of primate IBN spike trains using system identification techniques. II. Relationship to gaze, eye, and head movement dynamics during head-free gaze shifts. *J Neurophysiol* 78: 3283–3306, 1997b.

CULLEN KE AND MCCREA RA. Firing behavior of brain stem neurons during voluntary cancellation of the horizontal vestibuoocular reflex. I. Secondary vestibular neurons. *J Neurophysiol* 70: 828–843, 1993.

CURTHOYS IS, MARKHAM C, AND FURUYA N. Direct projection of pause neurons to nystagmus-related excitatory burst neurons in the cat pontine reticular formation. *Exp Neurol* 83: 414–442, 1984.

DU LAC S AND KNUDSEN EI. Neural maps of head movement vector and speed in the optic tectum of the barn owl. *J Neurophysiol* 63: 131–146, 1990.

EGGERT T AND KAPOULA Z. Position dependency of rapidly induced saccade disconjugacy. *Vision Res* 35: 3493–3503, 1995.

ERKELENS CJ, STEINMAN RM, AND COLLEWIJN H. Ocular vergence under natural conditions. II. Gaze shifts between real targets differing in distance and direction. *Proc R Soc Lond B Biol Sci* 236: 441–465, 1989.

FIORAVANTI F, INCHINGOLO P, PENSIERO S, AND SPANIO M. Saccadic eye movement conjugation in children. *Vision Res* 35: 3217–3228, 1995.

Downloaded from www.physiology.org/journal/jn at Johns Hopkins Univ Serials Dept Electronic (162.129.251.017) on July 26, 2019.

FREEDMAN EG AND SPARKS DL. Eye-head coordination during head-unrestrained gaze shifts in rhesus monkeys. *J Neurophysiol* 77: 2328–2348, 1997.

FREEDMAN EG, STANFORD TR, AND SPARKS DL. Combined eye-head gaze shifts produced by electrical stimulation of the superior colliculus in rhesus monkeys. *J Neurophysiol* 76: 927–952, 1996.

FUCHS AF AND ROBINSON DA. A method for measuring horizontal and vertical eye movements in the monkey. *J Physiol (Lond)* 191: 609–631, 1966.

GALIANA HL AND GUITTON D. Central organization and modeling of eye-head coordination during orienting gaze shifts. *Ann NY Acad Sci* 656: 452–471, 1992.

GOLDBERG ME. The control of gaze. In: *Principles of Neural Science* (4th ed.), edited by Kandel ER, Schwartz JH, and Jessell Norwalk TM. New York: Appleton and Lange, 2000, p. 782–800.

GRANTYN A AND GRANTYN R. Axonal patterns and sites of termination of cat superior colliculus neurons projecting in the tecto-bulbo-spinal tract. *Exp Brain Res* 465: 243–257, 1982.

GRANTYN A, GRANTYN R, GAUNITZ U, AND ROBINE KP. Sources of direct excitatory and inhibitory inputs from the medial rhombencephalic tegmentum to lateral and medial rectus motoneurons in the cat. *Exp Brain Res* 39: 49–61, 1980.

GREEN A AND GALIANA HL. Exploring sites for short-term VOR modulation using a bilateral model. In: *New Directions in Vestibular Research*, edited by Highstein SM, Cohen B, and Buttner-Ennever J. New York: Ann. NY Acad. Sci., 1996, vol. 781, p. 625–629.

HARRIS CM AND WOLPERT DM. Signal-dependant noise determines motor planning. *Nature* 394: 780–784, 1998.

HAYES AV, RICHMOND BJ, AND OPTICAN LM. A UNIX-based multiple process system for real-time data acquisition and control. *WESCON Conf Proc* 2: 1–10, 1982.

JUDGE SJ, RICHMOND BJ, AND CHU FC. Implantation of magnetic search coils for measurement of eye position: an improved method. *Vision Res* 20: 535–538, 1980.

KELLER EL, MCPEEK RM, AND SALZ T. Evidence against direct connections to PPRF EBNs from SC in the monkey. *J Neurophysiol* 84: 1303–1313, 2000.

KING WM AND ZHOU W. New ideas about binocular coordination of eye movements: is there a chameleon in the primate family tree? *Anat Rec (New Anat)* 261: 153–161, 2000.

KING WM, ZHOU W, TOMLINSON RD, MCCONVILLE KMV, PAGE WK, PAIGE GD, AND MAXWELL JS. Eye position signals in the abducens and oculomotor nuclei of monkeys during ocular convergence. *J Vestib Res* 4: 401–408, 1994.

LEIGH RJ AND ZEE DS. *The Neurology of Eye Movements* (3rd ed.). New York: Oxford, 1999, p. 286–320.

MAGNIN M, COURJON JH, AND FLANDRIN JM. Possible visual pathways to the cat vestibular nuclei involving the nucleus prepositus hypoglossi. *Exp Brain Res* 51: 298–303, 1983.

MAXWELL JS AND KING WM. Dynamics and efficacy of saccade-facilitated vergence eye movements in monkeys. *J Neurophysiol* 68: 1248–1260, 1992.

MAYS LE. Neural control of vergence eye movements: convergence and divergence neurons in midbrain. *J Neurophysiol* 51: 1091–1108, 1984.

MAYS LE. Has Hering been hooked? *Nature Med* 4: 889–890, 1998.

MAYS LE AND GAMLIN PDR. Neuronal circuitry controlling the near response. *Curr Opin Neurobiol* 5: 763–768, 1995a.

MAYS LE AND GAMLIN PDR. A neural mechanism subserving saccade-vergence interactions. In: *Eye Movement Research: Mechanisms, Processes and Applications*, edited by Findlay J, Walker R, and Kentridge RW. Amsterdam: Elsevier, 1995b, p. 215–223.

MAYS LE, PORTER JD, GAMLIN PDR, AND ELLO CA. Neural control of vergence eye movements: neurons encoding vergence velocity. *J Neurophysiol* 56: 1007–1021, 1986.

MCCONVILLE K, TOMLINSON RD, KING WM, PAIGE G, AND NA E-Q. Eye position signals in the vestibular nuclei: consequences for models of integrator function. *J Vestib Res* 4: 391–400, 1994.

MCCREA RA. The nucleus prepositus. In: *Neuroanatomy of the Oculomotor System*, edited by Buttner-Ennever JA. New York: Elsevier-Science Publishers, 1988, p. 203–223.

MUNOZ DP, GUITTON D, AND PÉLISSON D. Control of orienting gaze shifts by the tectoreticulospinal system in the head-free cat. III. Spatiotemporal characteristics of phasic motor discharges. *J Neurophysiol* 66: 1642–1666, 1991.

OOHIRA A. Vergence eye movements facilitated by saccades. *Jpn J Ophthalmol* 37: 400–413, 1993.

PHILLIPS JO, LING L, AND FUCHS AF. Action of the brainstem saccade generator during horizontal gaze shifts. I. Discharge patterns of omnidirectional pause neurons. *J Neurophysiol* 81: 1284–1295, 1999.

PHILLIPS JO, LING L, AND FUCHS AF. Burst activity in the primate PPRF during head-unrestrained gaze shifts. *NCM Abstract* 6: D-10, 2001.

PHILLIPS JO, LING L, FUCHS AF, SIEBOLD C, AND PLORDE JJ. Rapid horizontal gaze movement in the monkey. *J Neurophysiol* 73: 1632–1652, 1995.

ROY JE AND CULLEN KE. A neural correlate for vestibulo-ocular reflex suppression during voluntary eye-head gaze shifts. *Nature Neurosci* 1: 404–410, 1998.

SCUDDER CA AND FUCHS AF. Physiological and behavioral identification of vestibular nucleus neurons mediating the horizontal vestibuloocular reflex in trained rhesus monkeys. *J Neurophysiol* 68: 244–264, 1992.

SPARKS DL. Conceptual issues related to the role of the superior colliculus in the control of gaze. *Curr Opin Neurobiol* 9: 698–707, 1999.

STRASSMAN A, EVINGER C, MCCREA RA, BAKER RB, AND HIGHSTEIN SM. Anatomy and physiology of intracellularly labeled omnipause neurons in the cat and squirrel monkey. *Exp Brain Res* 67: 436–440, 1987.

STRASSMAN A, HIGHSTEIN SM, AND MCCREA RA. Anatomy and physiology of saccadic burst neurons in the alert squirrel monkey. I. Excitatory burst neurons. *J Comp Neurol* 249: 337–357, 1986a.

STRASSMAN A, HIGHSTEIN SM, AND MCCREA RA. Anatomy and physiology of saccadic burst neurons in the alert squirrel monkey. I. Inhibitory burst neurons. *J Comp Neurol* 249: 358–380, 1986b.

SYLVESTRE PA AND CULLEN KE. Quantitative analysis of abducens neuron discharge dynamics during saccadic and slow eye movements. *J Neurophysiol* 82: 2612–2632, 1999a.

SYLVESTRE PA AND CULLEN KE. Monocularly tuned discharge dynamics of abducens and brainstem inhibitor burst neurons during disjunctive saccades. *Soc Neurosci Abstr* 25: 1652, 1999b.

ZEE DS, FITZGIBBON EJ, AND OPTICAN LM. Saccade-vergence interactions in humans. *J Neurophysiol* 68: 1624–1641, 1992.

ZHOU W AND KING WM. Ocular selectivity of units in oculomotor pathways. In: *New Directions in Vestibular Research*, edited by Highstein SM, Cohen B, and Buttner-Ennever J. New York: Ann. NY Acad. Sci., 1996, vol. 781, p. 724–728.

ZHOU W AND KING WM. Premotor commands encode monocular eye movements. *Nature* 393: 692–695, 1998.

Downloaded from www.physiology.org/journal/jn at Johns Hopkins Univ Serials Dept Electronic (162.129.251.017) on July 26, 2019.